THE PENNSYLVANIA STATE UNIVERSITY
SCHREYER HONORS COLLEGE

DEPARTMENT OF BIOCHEMISTRY AND MOLECULAR BIOLOGY

# CLONING OF THE GENES ENCODING THE PROTEINS OF LIPOYL COFACTOR BIOSYNTHESIS IN MYCOBACTERIUM TUBERCULOSIS AND CHARACTERIZATION OF LIPOYL SYNTHASE

ABIGAIL KATHRYN HORSTMANN
Summer 2010

A thesis
submitted in partial fulfillment
of the requirements
for a baccalaureate degree
in Biochemistry and Molecular Biology
with honors in Biochemistry and Molecular Biology

Reviewed and approved* by the following:

Squire J. Booker
Associate Professor of Chemistry, Biochemistry and Molecular Biology
Thesis Supervisor

Joseph C. Reese
Professor of Biochemistry and Molecular Biology
Honors Adviser

Scott B. Selleck
Department Head, the Department of Biochemistry and Molecular Biology

* Signatures are on file in the Schreyer Honors College.

## ABSTRACT

In recent years, tuberculosis has risen in incidence to become the single most deadly infectious disease, killing approximately 3 million people globally each year. This is partly due to the almost extraordinary ability of the causative agent, *Mycobacterium tuberculosis*, to overcome antibiotics by developing resistance at the genetic level. This leaves the worldwide biochemical community scrambling to engineer new antibiotics with novel targets, rendering them capable of thwarting bacilli immune to the drugs currently in use. In an effort to contribute to this international quest, here we have focused on one biochemical pathway within *M. tuberculosis* believed to have potential as an antibiotic target: the *de novo* lipoic acid biosynthesis pathway. For each protein involved in this pathway - acyl-carrier protein (ACP), octanoyltransferase (LipB), and lipoyl synthase (LipA) - the corresponding gene was cloned. LipA was chosen for further analysis, and was subsequently expressed, purified, and characterized biochemically. Herein we have provided evidence to suggest that *Mt*LipA is analogous to *Ec*LipA with regard to its 2 $[4Fe\text{-}4S]^{2+}$ cluster catalytic center and its basic activity in the presence of substrate.

# TABLE OF CONTENTS

## LIST OF FIGURES

## LIST OF TABLES

# LIST OF ABBREVIATIONS

5'dA – 5' deoxyadenosine

5'dA• – 5' deoxyadenosyl radical

AdoMet – S-adenosyl-$_L$-methionine

ACP – acyl-carrying protein

AI – as-isolated

Amp – ampicillin

AMP – adenosine monophosphate

ATP – adenosine triphosphate

BCG – Bacille Calmette-Guérin vaccine

BioB – biotin synthase

BME – β-mercaptoethanol

BSA – bovine serum albumin

CoA – coenzyme A

DNA – deoxyribonucleic acid

DNTP – deoxyribonucleotide triphosphate

DTT – dithiothreitol

*Ec*LipA – *Escherichia coli* lipoyl synthase

EPPS – 3-[4-(2-hydroxyethyl)-1-piperazinyl]-propanesulfonic acid

EPR – electron paramagnetic resonance

EtBr – ethidium bromide

GCS – glycine cleavage system

HEPES – 4-(2-hydroxyethyl)-1-piperazineethanesulfonic acid

HIV – human immunodeficiency virus

HPLC – high performance liquid chromatography

INH – isoniazid

IPTG – isopropyl β-D-1-thiogalactopyranoside

Kan – kanamycin

KDa – kilo-Dalton

LAE – lipoate activating enzyme

LB – Leuria-Bertani

LCP – lipoyl-carrier protein

LipA – lipoyl synthase

LipB – octanoyl transferase

LipDH – lipoamide dehydrogenase

LT - lipoyltransferase

LplA – lipoate-protein ligase A

*Mt*LipA – *Mycobacterium tuberculosis* LipA

MDR-TB – multi-drug resistant tuberculosis

NAD+ - nicotinamide adenine dinucleotide

NADH – reduced nicotinamide adenine dinucleotide

NADPH – reduced nicotinamide adenine dinucleotide phosphate

Ni-NTA – nickel-nitrilotriacetic acid

nt – nucleotide

OD – optical density

PAS – *para*-aminosalicylic acid

PCR – polymerase chain reaction

PDC – pyruvate dehydrogenase complex

PFL-AE – pyruvate formate-lyase activating enzyme

PLP – pyridoxal-5-phosphate

POA – pyrazinoic acid

PZA – pyrazinamide

Pzase – pyrazinamidase

RCN – reconstituted

RFLP – restriction fragment length polymorphism

RMP – rifampin

RNA – ribonucleic acid

rRNA – ribosomal ribonucleic acid

SAM- S-adenosyl-$_L$-methionine

SDS – sodium dodecyl sulfate

SDS-PAGE – sodium dodecyl sulfate polyacrylamide gel

SM - streptomycin

sSNP – single-nucleotide polymorphism

TB – tuberculosis

TCEP – tris(2-carboxyethyl)phosphine

TDM – trehalose dimycolate

ThiH – tyrosine lyase

TPP – thiamine diphosphate (also known as TDP)

TraSH – transposon site hybridization

tRNA – transfer ribonucleic acid

UV-vis – ultraviolet-visible

WHO – the World Health Organization

XDR-TB – extensively drug-resistant tuberculosis

# ACKNOWLEDGEMENTS

First and foremost I would like to thank my thesis supervisor Dr. Squire Booker, for graciously allowing me to join his laboratory team for the duration of my research efforts. There are no words to adequately describe my gratitude for the opportunity he has provided me with, or the extent of what I have learned during my time in the Booker Lab. I experienced many firsts in that laboratory, some more character-shaping than others: my first encounters with liquid nitrogen, my first obstinate PCR, my first 20-hour day, my first protein purification (a success!), my first personal desk, and above all my first real biochemical research. I like to think that my time there turned me from a young and bungling undergraduate scientist-to-be into a young and *sometimes* bungling biochemist. I couldn't have made this transformation without your help.

Also key to the successful completion of this thesis, and thus my undergraduate career, was my honors adviser Dr. Joseph Reese. My adviser since I made the switch from chemistry to biochemistry, he has been there to offer advice (most critically in the area of choosing a graduate school) and support, and even sign the occasional form, when I needed it. Best of luck with all your future advisees! My appreciation also goes out to Dr. Carsten Krebs, whose knowledge and help – affably given – was essential for the Mössbauer portion of the experimentation that follows.

This brings me to Mr. Kyung-hoon Lee, without whom this thesis could not have come to fruition. A member of the Booker Lab, he was assigned the rather daunting task of guiding me through my experiments (most of which I had only read about before) and watching over my exploits, for better or worse, throughout my research. Being his

shadow for the first few months was a crash course in how to be a good scientist – careful, efficient, informed, persistent, and able to roll with the punches – and his abundance of knowledge and expertise will always be something I will try to strive for. Admittedly I wasn't always the perfect student, but he took my mistakes with stride and patience, and was able to answer virtually any question I could think to throw at him. Literally following in his footsteps day after day has taught me almost everything that I know in terms of biochemical technique, and for that I will forever be grateful. Kyung, it has truly been a privilege to learn from you, and I sincerely wish you the best in everything that you do.

A big thanks as well to the other members of the Booker Lab – your help big and small, as well as your tolerance of having an unpracticed hand working around your own experiments, was easily given. I apologize if at any point I was an inconvenience, but thank you for never treating me as one. I'm sure this is only the beginning of terrific scientific careers for all of you.

Lastly I must thank my friends and family who were always willing to lend an ear throughout this process, whether I was waxing optimistic or stressed. Your encouragement was invaluable to me, and I love you all.

## Chapter 1

# Introduction

"The Modern Crusade against tuberculosis brings hope and bright prospects of recovery to hundreds and thousands of victims of the disease who under old teachings were abandoned to despair." – Theodore Roosevelt

Throughout the history of human disease, the etiological agent of tuberculosis (TB) infection, *Mycobacterium tuberculosis*, has proved a formidable and sophisticated adversary. Today it has reached "superbug" status, responsible for more than 26% of all preventable adult deaths worldwide and considered the number one single infectious disease killer (1, 2). This feat is in direct defiance of the veritable cornucopia of antibiotics developed to fight its pathogenicity, as well as in spite of a vaccine in widespread use globally (3). *M. tuberculosis* has accomplished this through not only its natural prowess as a prokaryote, but also through progressive mutation rendering it resistant to increasing numbers of these anti-bacterial agents. Without the identification of new antibiotic targets and subsequent creation of novel drugs, TB will continue to ravage the human population, continuing to live up to the "global emergency" declared by the World Health Organization (WHO) 17 years ago (1).

## 1.1 The Unsolved Mystery of *M. tuberculosis* Evolution

Every organism has an evolutionary beginning – and for *M. tuberculosis*, those origins still remain contested. However, this does not include the mycobacterium's chronological beginnings, which were estimated more than a decade ago and remain unchallenged. Researchers van Embden *et al*. used genetic probes such as IS*6110* to produce restriction fragment length polymorphism (RFLP) patterns, through which they could examine strain differentiation (4). Their results indicated significant chromosomal heterogeneity among the species, a factor that, when coupled with the widespread global incidence of TB infection, suggested the organism was genetically diverse as well as relatively antediluvian.

Prompted to further examine the genetic variation of *M. tuberculosis*, scientists Kapur and his colleagues conducted genomic studies that showed surprisingly low nucleotide variance between TB mycobacteria collected worldwide. Based on this, as well as drug resistance studies that reported a spontaneous mutation frequency within the range found for the majority of other bacterial species, Kapur *et al*. threw out the possibility of the organism having exceptional deoxyribonucleic acid (DNA) replication fidelity or DNA repair (5,6). Instead they compared nucleotide variation rates of *M. tuberculosis* to *Escherichia coli* and *Salmonella typhimurium*, organisms whose date of evolutionary divergence had already been estimated (7). Their calculations found that the speciation of *M. tuberculosis* occurred 15,300-20,400 years ago, making it a relatively recent addition to the pathogen roster contrary to prior speculation (7).

It is the progenitor from which TB bacteria arose that still eludes scientists. Aiding in the identification of this ancestor is *M. tuberculosis*'s membership in the *Mycobacterium tuberculosis* complex, a group of closely-related mycobacterium species including *M. bovis, M. bovis* BCG, and *M. africanum*, as well as the rarely-seen *M. caprae, M. microti, M. canettii,* and *M. pinnipedii* (8). The mycobacteria of this group have been found to have a greater than 99.9% sequence similarity as well as identical 16S ribosomal ribonucleic acid (rRNA) sequences, though they each exhibit different pathogenicity, host preferences, epidemiology, drug sensitivity and geographic range (8,9,10).

Initial hypotheses of *M. tuberculosis* evolution took into account the domestication of animals roughly 10,000-25,000 years ago, speculating that *M. bovis* bacteria were transmitted from cattle to humans during this time period (11). Subsequent adaptation of the *M. bovis* bacteria, which are responsible for TB-like disease in bovines, to their new human hosts, could theoretically have resulted in the first *M. tuberculosis* cells. Analysis of *M. bovis* and *M. tuberculosis* synonymous single-nucleotide polymorphisms (sSNP) has provided a competing theory: that the two evolved in parallel (12). The most recent and convincing hypothesis, put forth by scientists Brosch *et al*. as a result of their examination of deletion and insertion mutations in *M. tuberculosis* complex genomes, theorizes that both mycobacteria species developed independently from a precursor species, perhaps related to *M. canetti* (13).

## 1.2 Pathogen Meets Human: a Brief History of Tuberculosis Infection

No matter how TB disease first came into being, the fact remains that it has been plaguing human populations for thousands of years, as proven by analysis of preserved bone tissue. The first biologically evidenced cases of TB have been traced to ancient pharoic Egypt, where scientists have identified *M. tuberculosis* presence in 4,000 year-old mummified bones through spoligotyping technique (14). Similar bone-presence has also been detected in Neolithic sites in Italy, Denmark, and several Middle Eastern regions, providing further substantiation of a global TB presence at least 4,000 years ago (9).

Indeed the history of mankind has been fraught with TB affliction, though it has gone by many different names. It appears in the scripture of the Bible under the name "consumption", and in writings by famed Greeks Hippocrates and Aristotle (circa 400 BC and 350 BC, respectively) by the calling card "phthisis" – Greek for "to waste away" (15). The 200 year-old outbreak in Europe beginning in the 1600's, known as the "Great White Plague" was responsible for about 25% of the deaths at time, and was also a large-scale manifestation of TB (9).

Scientists and physicians alike remained in the dark as to the disease's cause until the late 1800's – by which time TB was claiming one in seven lives in Europe and the Americas (15). In 1882, German biologist Robert Koch announced his groundbreaking discovery, forever silencing the common beliefs that TB occurred spontaneously within the unlucky, or was passed genetically. Against all odds, as *M. tuberculosis* is notoriously difficult to work with even today, Koch had identified TB as an infectious disease and

had isolated the etiological agents responsible: tubercle bacilli (16). The news of Koch's discovery spread quickly, bringing the hope of an eventual cure to patients and researchers alike. More significantly, his reports of a hitherto unheard-of contagious agent acted as a catalyst for a cascade of antibiotic developments that have left a trail of antibiotic resistance in their wake, despite their initial success.

### 1.3 Antibiotic Resistance: the Deadly Sidekick to *M. tuberculosis*

To date, *M. tuberculosis* has confounded the world with its ability to elude antibiotic suppression. Were it not for this aptitude, the success seen in the first antibiotic trials may not have faded. The enthusiasm that greeted the first two effective anti-tuberculosis antibiotics, streptomycin, discovered by Albert Schatz and Selman Waksman in 1943, and *para*-aminosalicylic acid (PAS), by Harold Lehmann, was resounding (17,18). This was partially because *M. tuberculosis* had already defied the previously developed antibiotics, sulfonamides and penicillin (19). The first blow to this euphoria was when the majority of patients treated with streptomycin monotherapy began to relapse, and could no longer be improved upon administration of the drug that once helped them. Treatment with one drug alone created an environment that was selective for resistant bacteria, thus encouraging the growth of mutated mycobacteria populations. It was found that the emergence of antibiotic resistance could be avoided through combination therapy with streptomycin and PAS (20). Since then, the contemporary drugs isoniazid, pyrazinamide, rifampin, and ethambutol have all been discovered and put into widespread use in combination therapies. These antibiotics, in combination with the

knowledge of resistance development gained from the streptomycin monotherapy failure provide the necessary tools to combat TB. Unfortunately circumstances such as inadequate therapy, often in the form of poor adherence, and the compartmentalization of infection that occurs during TB disease progression, are in effect creating a monotherapy-type environment for the mycobacteria (19). In this way, resistance has developed to almost every antibiotic currently in widespread use, which is most notably seen in the growing global reservoirs of multi-drug resistant TB (MDR-TB) and, even more menacing, extensively drug-resistant TB (XDR-TB).

**Inherent resistance of the bacilli: the mycobacterial cell wall**

The array of resistance mechanisms in the arsenal of *M. tuberculosis* is persistently growing and its true extent remains unknown. Though much of this can be attributed to mutations in the mycobacterium's genome, the organism is intrinsically blessed with an inimitably resistant cell wall, different from those of both Gram-positive and Gram-negative bacteria. As can be seen in Figure 1-1, the cell walls of all three types of bacteria are comprised of a lipid bilayer, periplasmic space, some amount of peptidoglycan, and polysaccharide side-chains. However, only mycobacteria and Gram-negative bacteria possess lipids exterior to the peptidoglycan layer (21).

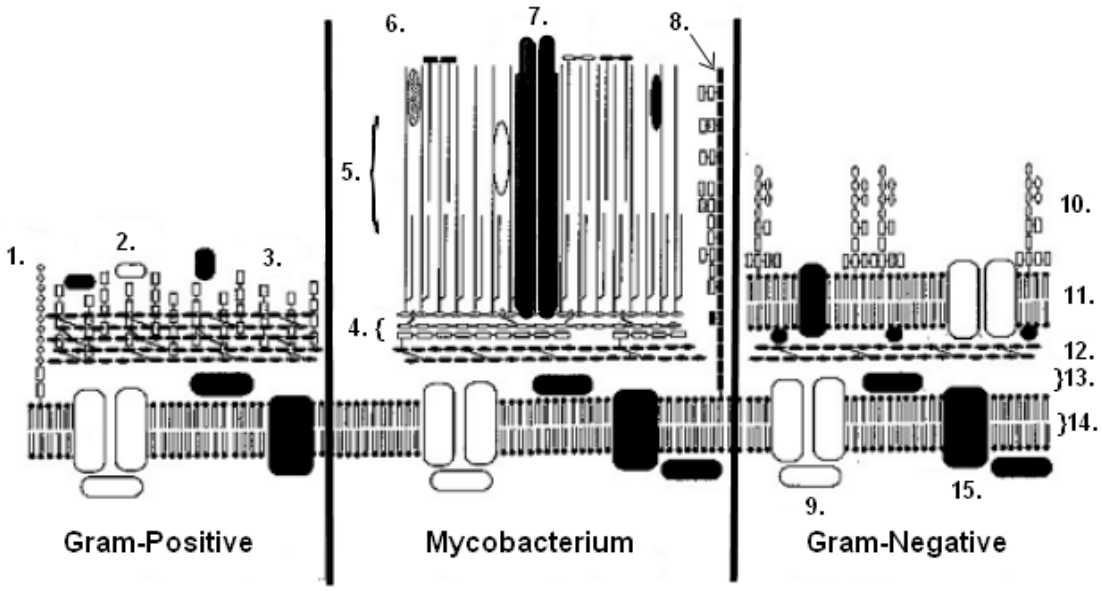


Figure **1-1**: Illustrational models of gram-positive, mycobacterial, and gram-negative cell envelopes and their corresponding components. The constituents depicted here include lipoteichoic acids (1), surface proteins (2), teichoic acids (3), arabinogalactan (4), mycolic acids (5), free wall glycolipids and proteins (6), an outer porin (7), lipoarabinomannan (LAM) (8), inner porins (9), lipopolysaccharide (LPS) (10), outer membrane (11), peptidoglycan (12), periplasmic space (13), cell membrane (14), and membrane-associated proteins (15).

Traveling outward past this point in the mycobacterium's cell envelope, one can see how truly distinguished the microorganism's protective layers are. Attached to the peptidoglycan covalently via a unique diglycosylphosphoryl bridge, is a mycolyl-arabinogalactan macromolecular structure composed of mycolic acid, an alpha-branched fatty acid, and arabinogalactan, a complex polysaccharide (22). The mycolic acids are orientated perpendicularly to the membrane plane, creating a singular lipid barrier that acts as a key component of the disease-inducing aspects of *M. tuberculosis* and controls the permeability of the cell surface (23). Because mycolic acids are long-chain, branched, and contain few double bonds, this arrangement fashions a highly hydrophobic layer of low fluidity that is capable of rebuffing hydrophilic compounds, such as antibiotics (21).

Though the mycobacterial cell wall contains porin-like proteins that can act as aqueous channels for hydrophilic agents, they are relatively inefficient and are present in only low concentrations, contributing to the cell's low permeability (24).

Another significant feature of the mycobacterium's outer layers is the high presence of trehalose dimycolate (TDM). TDM is a surface glycolipid otherwise known as "cord factor," as it is responsible for the distinctive serpentine cord formation assumed by plated *in vitro*-grown *M. tuberculosis* colonies (25) (Figure 1-2). TDM is a strong indicator of strain virulence, as it is toxic to mammalian cells, inhibits the migration of polymorphonuclear leukocytes and assumes control of macrophages via activation of a focal adhesion kinase (25,26). The combination of resistance- and virulence-bestowing lipids on the surface of *M. tuberculosis* has undoubtedly proved to be a highly effective combination in the organism's face-off with the human immune system. The upside to such a remarkable cell envelope is that it provides a rich collection of drug targets: those enzymes crucial to the biogenesis of the cell wall structure and its components.

Figure **1-2**: Colonies of *M. tuberculosis* grown on Lowenstein-Jensen media exhibiting the cording growth patterns characteristic of virulent strains. Image obtained from Todar's Online Textbook of Bacteriology (25).

**Acquired resistance: TB antibiotics and the mutations that circumvent them**

Streptomycin, the first anti-tuberculosis drug, was also the first to be met with enough bacterial resistance to render it useless, even problematic, as a monotherapy. As an aminoglycoside, streptomycin interferes with bacterial cell life by binding irreversibly to the ribosome at the S12 protein of the 30S subunit, preventing the binding of formyl-methionyl-tRNA (Figure 1-3) (27). This blockage causes misreading of the genetic code, inhibition of initiation of protein synthesis, and faulty proofreading, thus killing the target cell during its growth phase (Figure 1-4) (21). However, because *M. tuberculosis* only has one copy of rRNA genes, a single mutation can destroy streptomycin's effectiveness (1). The mutations most commonly associated with streptomycin resistance have been identified in the *rpsL* gene, particularly at codons 43 and 88, and the 16S rRNA gene (*rrs*) in the regions surrounding nucleotides 530 and 951 (1). The *rspL* gene is responsible for encoding the S12 protein subunit (21). As a result of the relatively high (and growing) rate of resistance to streptomycin, as well as its occasional ototoxic side effects, streptomycin is currently considered a second-line TB antibiotic, relinquishing the spotlight to first-line TB-fighters isoniazid, pyrazinamide, rifampin, and ethambutol (Figure 1-4).

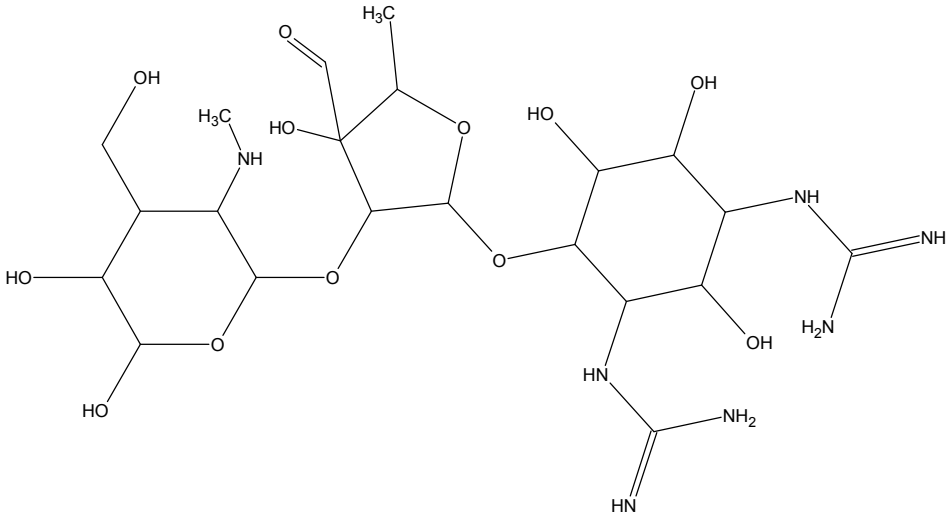


Figure **1-3**: The structure of the aminoglycoside streptomycin, the first anti-TB antibiotic put into widespread use.

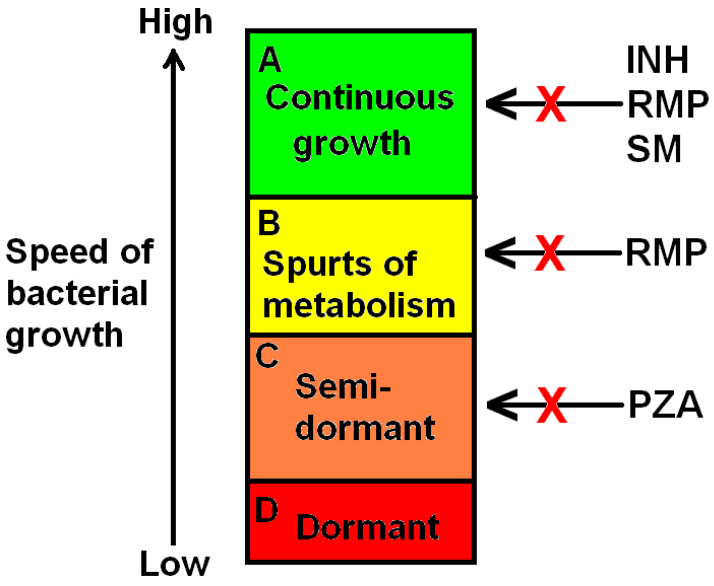


Figure **1-4**: Hypothesized action of several anti-TB drugs with respect to when they act in the lifecycle of the tubercle bacilli. Isoniazid (INH), as well as rifampin (RMP) and streptomycin (SM), are able to act against actively growing organisms (a). Pyrazinamide (PZA) inhibits semi-dormant organisms through the creation of an acidic environment (b). Rifampin also acts against semi-dormant organisms, particularly those that exhibit spurts of active metabolism (c). In the completely dormant stage, the bacilli are immune to the action of any of these drugs (d).

The first of these to be discovered, isoniazid, was by coincidence discovered in three different labs in a short time period spanning 1951 and 1952. The first to unearth it by a margin of only a few weeks, Harry Yale, did so purely by accident whilst in the process of investigating the antibacterial effects of another compound, thiosemicarbazone, for which isonicotinic acid is an intermediate (28). A synthetic antibiotic whose chemical structure is shown in Figure 1-5, isoniazid acts primarily by impeding the oxygen-dependent steps of mycolic acid biosynthesis (29). Such inhibition severely compromises the mycobacterial cell wall and renders it vulnerable to the hostile environment within the host. The precise mechanism of isoniazid remained unknown until research by Banerjee *et al*. examined isoniazid-resistant strains via a cell-free mycolic acid synthesizing system (30). Their results revealed that isoniazid targeted the product of the *inhA* gene, a protein that catalyzes NADH-dependent reduction of delta-*trans*-enoyl thioesters of either CoA or acyl CoA (31). Obstruction of this enzyme is deleterious to fatty acid elongation, and through this action isoniazid was found to be 15 times more potent than streptomycin (28). Despite this efficacy, isoniazid is also a victim of resistance; resistant bacteria have been identified with mutations in not only the *inhA* gene, but also single or multiple mutations in *katG, aphC*, and various hitherto unidentified genes (1).

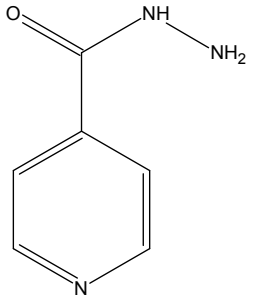


Figure **1-5**: The chemical structure of isoniazid, a derivative of nicotinic acid capable of inhibiting actively growing *M. tuberculosis* bacteria.

Pyrazinamide, an isostere of isoniazid (as well as another derivative of nicotinic acid) was the next to be associated with anti-TB activity, circa 1952 as a result of work by Kushner *et al*. (Figure 1-6) (32). A diazine carboxamide, pyrazinamide had first been synthesized in 1936 as a possible analeptic, or central nervous system stimulant (28). By targeting older, semi-dormant tubercle bacilli, pyrazinamide is able to shorten the required length of TB therapy from 9-12 months to 6 months (28,33). As an antibacterial agent, it is only active at acidic pH, which corresponds to the environment generated during active inflammation (34,35). This acidic pH requirement is due to the action of pyrazinamide: at low pH, the mycobacterium's own nicotinamidases/pyrazinamidases (PZases) convert pyrazinamide into its active form, pyrazinoic acid (POA). In this form, POA is able to collapse the cell membrane potential, thus affecting membrane transport (1). *M. tuberculosis* exhibits particular susceptibility to pyrazinamide due to its naturally poor POA efflux mechanism (34). Unfortunately, pyrazinamide too has encountered resistant bacilli. Those mycobacteria with mutations in the gene encoding pyrazinamidase, *pncA*, especially codons 63, 138, 141, and 162, were found to possess immunity to pyrazinamide action (1). Recent experimentation by Unissa and colleagues

suggests that the most effective mutations in the *pncA* gene create a mutant pyrazinamidase with altered folding or positioning of the catalytic residue side chains (36). Without a normally functional pyrazinamidase enzyme, pyrazinamide would remain in its inactive form and be unable to de-energize the membrane. Additionally, thus far mutations in *pncA* have failed to account for resistance in 28% of pyrazinamide-resistant isolates, suggesting that another gene contributes to this form of resistance (1).

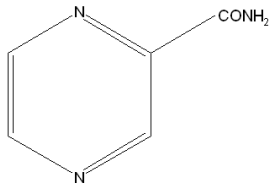


Figure **1-6**: The structure of the antibiotic pyrazinamide, isostere to isoniazid, that acts against tubercle bacilli through acid inhibition.

Another first-line antibiotic, Rifampin, was isolated from a fermentation broth of *Streptomyces mediterranei* by Sensi and colleagues in 1959 (28,37). This compound is a semi-synthetic derivative of rifamycin B, divergent from its parent molecule in its antibacterial capabilities (Figure 1-7) (38). Capable of readily diffusing across the mycobacterial membrane, rifampin is highly bactericidal and thus one of the most important members of the current anti-TB drug cocktail (1). Upon treatment with rifampin, the elongation step of DNA-dependent transcription by RNA polymerase is blocked in susceptible mycobacteria (21). Almost the entirety of rifampin-resistant *M. tuberculosis* bacteria isolates, in fact 96%, have been found to have mutations in a central 81-base pair (27 codon) region of the *rpoB* gene, which encodes the β-subunit of RNA polymerase (1,19,21,39). It should be noted that not all mutations within the 81-base pair region are created equal. Deviance from the wild-type base pair sequence at codons 526

and 531 has been found to bestow particularly high levels of resistance to rifampin, while mutations at codons 511, 516, 518, and 522 yield an organism with low levels of resistance to rifampin and another derivative of rifamycin (rifapentin) but that is still vulnerable to two other rifamycins (rifabutin and rifalazyn) (40). Interestingly, occurrence of rifampin monoresistance is rare, which means resistance to rifampin can function as a valuable surrogate marker of multi-drug resistance (41).

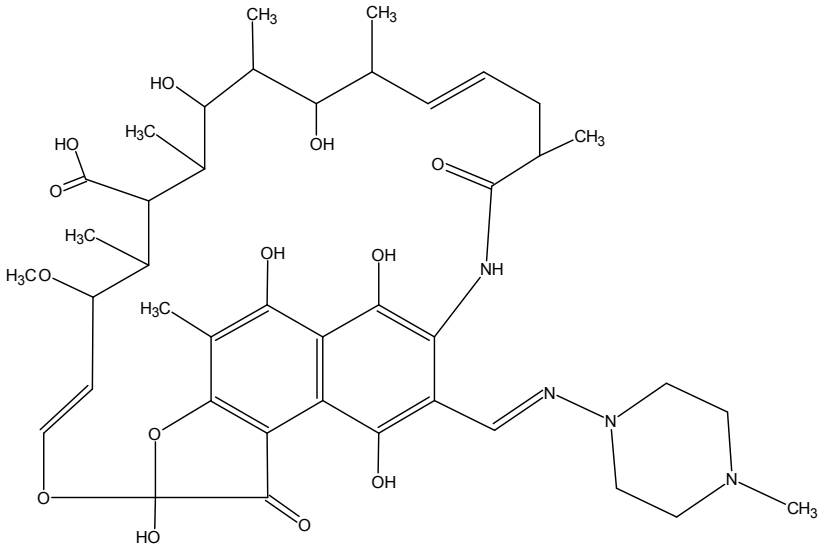


Figure **1-7**: The rifampin molecule that as a part of the anti-TB drug regimen, acts as an inhibitor of RNA polymerase.

Ethambutol was the fourth and final drug to join the ranks of the first-line TB drugs, completing the quartet that remains so heavily in use today (Figure 1-8). This bactericidal compound is a derivative of ethylenediamine in which every nitrogen atom is bound to the α-carbon of n-butanol (Figure 1-9) (28). Upon its creation in 1961 by researchers at Lederle Laboratories, ethambutol's dextrorotatory enantiomer was reported to have four times the antibiotic activity of streptomycin, as well as to possess activity against strains of *M. tuberculosis* that were already isoniazid- and streptomycin-resistant

(42). Ethambutol is currently thought to obtain its effectiveness by posing as an arabinose analog able to interact with arabinosyl transferase, and in this way preventing the transfer of arabinose to the cell wall acceptor (1,43). Thus the polymerization of cell wall arabinan is inhibited, resulting in the accumulation of decaprenol phosphoarabinose, a lipid carrier (44,45). In 1997 scientists Telenti *et al*. reported that through examination of ethambutol-resistant mycobacteria they had identified the gene cluster: *emb*CAB (43). This genetic region had just previously been reported to encode for mycobacterial arabinosyl transferases by Belanger *et al*. in their work with *M. avium* (46). It was found that 69% of all resistant strains were mutated in *embB*, 98% of whom had a mutation at codon 306 – an amino acid substitution that wasn't observed in susceptible isolates (1,43). However, the resistance observed in the other 30% of resistant *M. tuberculosis* still remains to be explained.

| Extent of activity | Prevention of resistance | Early bactericidal | Sterilizing |
|---|---|---|---|
| **High** | isoniazid, rifampin | isoniazid | rifampin, pyrazinamide |
| | ethambutol, streptomycin | ethambutol, rifampin | isoniazid |
| **Low** | pyrazinamide | streptomycin, pyrazinamide | streptomycin, ethambutol |

Figure **1-8**: The relative activities of the five major antibiotics in use against tuberculosis bacteria.

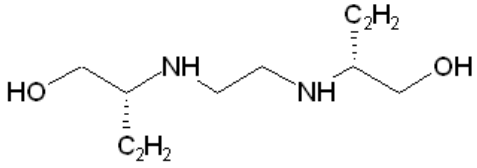

Figure **1-9**: The chemical structure of ethambutol, which allows it to act as an analog of arabinose in its interaction with arabinosyl transferase.

## 1.4 The Bacille Calmette-Guérin Vaccine: Not Quite What the Doctor Ordered

The current anti-TB vaccine in use, the Bacille Calmette-Guérin (BCG) vaccine, has been administered more times than any other vaccine in the history of the world (47). Seemingly in contradiction to this fact, BCG leaves much to be desired in terms of protection against TB infection, and isn't even in use in the United States. First used in humans in 1921 after its invention by French scientists Calmette and Guérin, BCG is a strain of live *M. bovis*, attenuated through 13 years of growth and 230 cultural passages on artificial media (originally a glycerin-bile-potato mixture) such that it no longer retains its virulence in humans (28). BCG is given to approximately 100 million newborns each year, reaching more than 80% of neonates and infants in countries that have implemented BCG at a national level (47,48). In this context, BCG is successful in preventing miliary and meningeal TB in young children. On the other hand, BCG is woefully inefficient in protecting where it is needed most: the most prevalent disease form, adult pulmonary disease (47). Its efficacy in this regard ranges from 0% in South India to 80% in the United Kingdom, and although meta-analysis has yielded an estimated overall efficiency rate of 50%, other claculations have concluded that just 5% of the total vaccine-preventable deaths caused by TB could even have been prevented by BCG vaccination

(3,49). Additionally, the majority TB cases arise when latent *M. tuberculosis* bacilli arise within their unaware host, and BCG can do nothing for those who are already inhabited by the mycobacteria (50).

### 1.5 Minuscule Microbes, Colossal Consequences

Today, *M. tuberculosis* is operating at a level of sophistication all its own, startling the world with its repeated success during a time of unprecedented medical technology, research, and development. These remarkable yet villainous bacilli have managed to thwart man, antibiotic, and vaccine alike.

The statistics currently surrounding the TB epidemic are truly staggering. As it stands today, about one third of the entire global population, or in other words, upwards of 2 billion people, are infected with latent TB, with one new infection *every second*. The National Foundation For Infectious Disease reports that of these, 5-10% will develop the active form of the disease (51).Yearly, approximately 3 million are lost to the disease, and in 2005, approximately 8,000 individuals lost their lives every day to TB. This epidemic is now the leading killer of women, the infectious disease that creates the most orphans, and the number one cause of death among those infected with human immunodeficiency virus (HIV). Most frightening of all is the gradual and inexorable spread of resistant TB microbes.

In 2009, the WHO estimated that there were 500,000 new cases of MDR-TB, or *M. tuberculosis* strains resistant to at least rifampin and isoniazid, in 2007 (52). This was accompanied by approximately 110,000 deaths attributed to MDR-TB in that year alone.

However, MDR-TB seems docile when compared to the even more nefarious XDR-TB, which is characterized by bacilli immune to not only first-line drugs, but second-line drugs as well. The WHO warns that if immediate action is not taken to suppress the proliferation of XDR-TB, these new superbugs will take humanity back to a vulnerability rivaling that of the pre-antibiotic age.

Without an effective vaccine, and with the gradual fall of the primary chemotherapy agents, the world is desperately in need of some new weapons with which to fight back. The range of research currently ongoing to fulfill this precise purpose is extensive enough to surpass the bounds of this paper, as scientists worldwide are answering the call to arms. The primary goal for those seeking to develop new TB therapies is to first unearth an antibiotic target that has never before been acted against, and therefore remains an Achilles' Heel in even the most foreboding of *M. tuberculosis* microorganisms.

### 1.6 Lipoic acid biosynthesis: a promising target

The key in finding such a target lies in the identification of a compound that carries out an essential function in the bacterial life cycle. In this respect, lipoic acid has the potential to fit the bill. Functioning as a simple yet crucial biochemical cofactor in several primary metabolic pathways, lipoic acid is conserved in eukaryotes and prokaryotes alike (53). The elucidation of the biosynthesis mechanisms of lipoic acid and the enzymatic reactions it participates in have revealed the nature of the compound's

cellular presence: knowledge that paves the way for its future medical application in *M. tuberculosis*.

## 1.7 The Beginnings of Lipoic Acid Investigation

Before lipoic was known by its current name, it went by two different calling cards, indicative of the ways by which the compound was discovered. One group, comprised of researchers Gunsalus *et al*., identified it during their investigations into the necessary growth factors of *Streptococcus faecalis*, an Enterococci, and dubbed it "the pyruvate oxidation factor" as a result of its role in the oxidative decarboxylation of pyruvate (54,55). Yet another set of scientists, working at the Lilly Research Laboratories, knew it as "acetate-replacing factor" as per its capability of taking the place of acetate in the growth media of certain lactic acid bacteria (56). Collaboration between the two groups led to the first isolation of the compound, a pale-yellow crystalline solid, by Lester Reed (then associated with the Lilly group) in 1951. This process involved a 300,000-fold purification, in which just 30 mg of lipoic acid crystals were obtained from an estimated starting point of 10 tons of liver residue. Subsequently, characterization of the newly isolated α-lipoic acid ensued.

## 1.8 Structure and function of lipoic acid and the lipoyl cofactor

Today, it is known that lipoic acid (6,8 thioctic acid, or 1,2-dithiolane-3-pentanoic acid) is a fatty acid comprised of eight carbons, with sulfurs at C-6 and C-8 in the form of

a cyclic disulfide (53,57) (Figure 1-10). *In vivo*, lipoic acid adopts its R-enantiomer form, and is biologically active when covalently attached to a lipoyl-carrier protein (LCP). This protein-bound form acts as a swinging arm of large multifunctional enzyme complexes, responsible for conveying substrates from one catalytic protein domain to the next. In this reaction the lipoyl cofactor is reductively converted from a lipoamide to a dihydrolipoamide (Figure 1-10) (58). The enzyme lipoamide dehydrogenase reverses this process, oxidizing the sulfur atom duo while simultaneously reducing NAD+ to NADH (59). Furthermore, the lipoic acid that remains unbound within an organism has extensive capabilities as a free antioxidant – able to chelate metals, scavenge reactive oxygen species, repair oxidative damage, and regenerate other endogenous antioxidants (60). The antioxidant prowess of lipoic acid can even be further extended by its reduction into the dihydrolipoic acid form. However, little free lipoate is present within the cell, and for the most part it exists in its protein-bound form, linked to the ε-amino terminus of a conserved lysine residue (61).

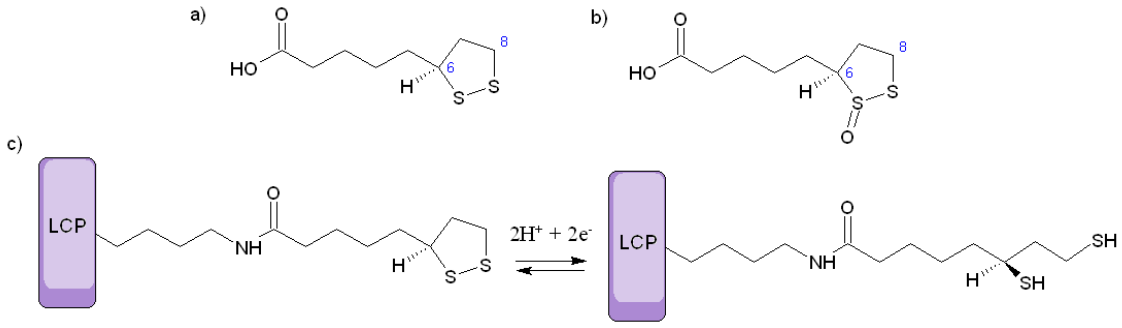


Figure **1-10**: The structures of α-lipoic acid (a) and β-lipoic acid (b). The swinging lipoyl arm attached to a LCP (c) is the form assumed by lipoic acid in its essential metabolic role as a redox cofactor.

## 1.9 The Starring Metabolic Role of Lipoic Acid

The essentiality of lipoic acid occurs in its role as a redox cofactor in the aforementioned enzyme complexes. Though the actual chemical action of the lipoyl cofactor is nothing exceptional, its function as part of a greater catalytic machine is invaluable to the cell. Lipoic acid acts as a key lipoyl cofactor in at least five vital metabolic processes and complexes: the glycine decarboxylase complex, the α-ketoglutarate dehydrogenase complex, the branched-chain oxo-acid dehydrogenase complex, the acetoin dehydrogenase complex, and, in it's most illustrious role of all, the pyruvate dehydrogenase complex.

### The glycine cleavage system

The glycine cleavage system (GCS) encompasses a set of proteins that carry out a sequence of metabolic processes in response to high concentrations of the amino acid glycine. Together, they cleave excess glycine into ammonia, carbon dioxide, and 5,10-methylenetetrahydrofolate to create a secondary pathway for the biosynthesis of one-carbon entities (53, 88). The first step in this process is carried out by the glycine decarboxylase complex, a four-protein system found in both prokaryotes and eukaryotes (Figure 1-11) (62). Klein, Sagers, and coworkers were the first to separate and identify all four proteins of the complex quartet through extensive study of the GCS in *Peptococcus glycinophilus*: the P-, H-, L-, and T-proteins. Equipped with the ability to isolate the

separate proteins, Kukuchi *et al*. were then able to determine the mechanistic action of the components of the complex (63). They found that the homodimeric P-protein, a pyridoxal phosphate (PLP) enzyme, is the first to act, decarboxylating the glycine molecule. The product of this primary reaction, a methylamine, reduces the lipoyl cofactor located on the H-protein by binding to a thiol group. The monomeric T-protein then steps in, removing a methylene residue, attaching it to tetrahydrofolate, and releasing ammonia and the reduced lipoyl H-protein. Lastly, the swinging arm of the lipoyl cofactor is regenerated via NAD+-dependent oxidation by the L-protein, a lipoamide dehydrogenase. The complex is then ready to process glycine once more.

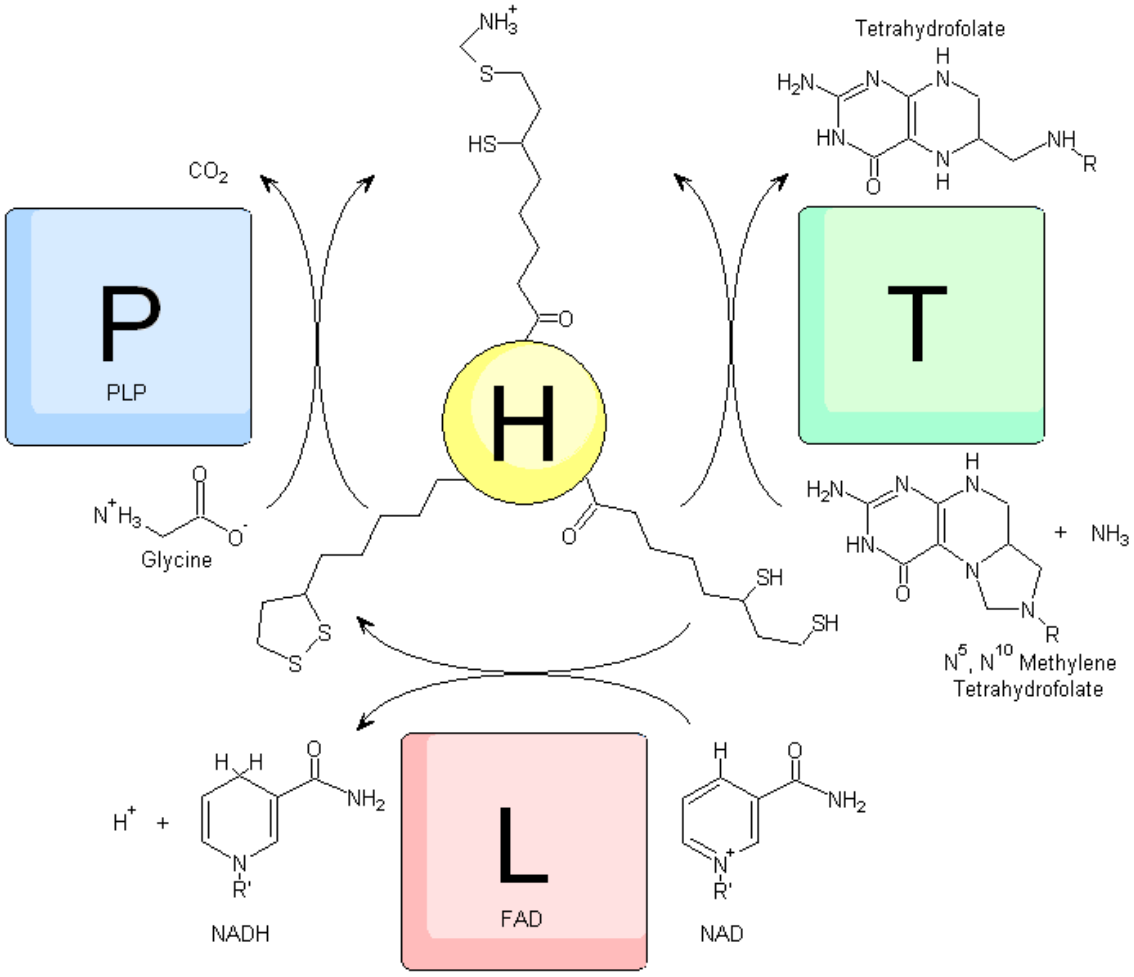


Figure **1-11**: A schematic representation of the glycine cleavage system. The swinging lipoyl cofactor arm can be seen attached to the H protein.

## The α-ketoglutarate dehydrogenase complex and the branched-chain oxo-acid dehydrogenase complex

Two more lipoyl-dependent enzyme complexes, the α-ketoglutarate dehydrogenase complex and the branched-chain oxo-acid dehydrogenase complex, act in a similar enough manner to be discussed in unison, though they have different functions:

of the decarboxylation of α-ketoglutarate, and the oxidative decarboxylation of α-keto acids, respectively (53). Both have three protein subunits (E1, E2, and E3). The E1 protein is a thiamine phosphate (TPP)-dependent α-ketoacid decarboxylase that reduces the lipoyl cofactor swinging arm of the E2 subunit through acylation (64,65). Both E1 and E3 are attached to the E2 subunit center, which has one or multiple lipoyl domains. Akin to the action observed in the glycine decarboxylase complex, the lipoyl domain delivers an acyl moiety to coenzyme A before being re-oxidized by a flavin-dependent protein (in this instance, the E3 subunit) for its re-use in additional cycles (66).

**The acetoin dehydrogenase complex**

Some fermentative bacteria are known to contain the acetoin dehydrogenase complex, which carries out the process of converting the neutral molecule acetoin into energy (and thus circumventing the need for another source of carbon). Recently, for the first time this enzyme complex was identified in an archaeon, *Sulfolobus solfataricus* (67). In terms of mechanistic action, this complex is analogous to the α-ketoglutarate dehydrogenase complex: the E1 subunit catalyzes cleavage of acetoin to acetaldehyde with subsequent transfer of an acetyl group to the lipoyl cofactor on E2, the E2 subunit bears dihydrolipoamide acyltransferase activity, and E3, as a dihydrolipoamide dehydrogenase, re-oxidizes the dihydrolipoyl group (68).

**The pyruvate dehydrogenase complex**

Finally, lipoic acid carries out its most illustrious function of all in the pyruvate dehydrogenase complex (PDC). The PDC uses a lipoyl cofactor in its catalysis of oxidative decarboxylation of pyruvate to form acetyl-CoA, a conversion crucial to aerobic respiration. As an enzymatic complex, the PDC is a trio of noncovalently associated proteins, similar to the α-ketoglutarate dehydrogenase and branched-chain oxo-acid dehydrogenase complexes, and is present in both prokaryotes and eukaryotic mitochondria (68). The E2p subunit, a dihydrolipoyl transacetylase, is located centrally, shuttling intermediates between the E1p and E3 subunits (a pyruvate dehydrogenase and dihydrolipoyl dehydrogenase, respectively) (Figure 1-12) (66,69). E1p utilizes a TPP cofactor in its oxidative decarboxylation of pyruvate, the first leg of the multistep reaction catalyzed by the PDC. This releases carbon dioxide and 2-hydroxyethylidene-TPP, the carbanion of which in turn reduces the E2p lipoyl cofactor, regenerating TPP and producing an acetyl-dihydrolipoamide. As seen in the other complexes, the lipoyl cofactor passes off the acetyl group to CoA (creating acetyl-CoA), leaving the reduced dihydrolipoyl structure. This is re-oxidized through the reduction of NAD+ to NADH by E3, resurrecting the active form of the enzyme for additional catalysis. In this way, the enzymes of the PDC act in a concerted manner to provide the central metabolic compound acetyl-CoA.

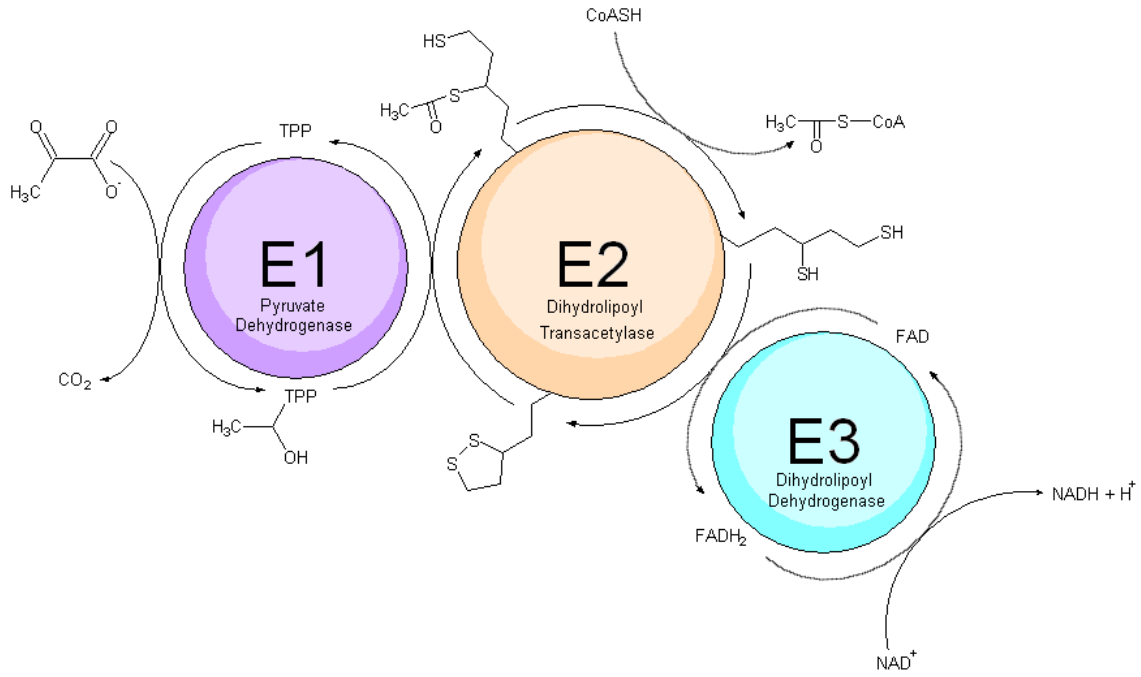


Figure **1-12**: Schematic representation of the action of the pyruvate dehydrogenase complex and the swinging lipoyl cofactor covalently attached to protein E2.

As a lipoyl cofactor in these primary metabolic processes, lipoic acid has proved itself indispensable. Due to this range of intracellular roles, if a cell, say a mycobacterium, were to lose the ability to synthesize the acid, theoretically that would be equivalent to losing the ability to survive. Thus, the lipoic acid biosynthesis pathway has garnered significant interest.

## 1.10 The Dual Pathways of Lipoylation

Because of the fundamental part played by cellular lipoyl cofactor, it is logical that most organisms have adopted a "don't put all your eggs in one basket" mentality, and thus employ more than one pathway for the ligation of lipoyl groups to apoprotein. Study in the Cronan laboratory has proven the existence of two separate pathways of lipoylation in *E. coli* (70). These redundant synthesis methods differ in not only the enzymes involved, but in their basic mechanism: exogenous uptake versus endogenous creation (Figure 1-13).

The lipoic acid salvage pathway allows the cell to directly uptake lipoic acid in its immediate surroundings. Upon reaching the cytoplasm, the lipoic acid is attached to the lysine residue of a waiting LCP in a two-step ATP-dependent process. First, the lipoic acid is activated by ATP, creating a lipoyl-AMP intermediate, and it is subsequently attached to the apoprotein, releasing AMP (70). This reaction necessitates two enzymes in mammalian cells, one, a lipoate activating enzyme (LAE), and the other, a lipoyltransferase (LT) (71). Conversely, in *E. coli* this is accomplished through the solo activity of lipoate-protein ligase A (LplA) (70).

*E. coli*'s other option is more involved, requiring the concerted action of three proteins rather than just one. This pathway begins with a lipoic acid precursor, a fatty octanoyl chain, attached by a thioester bond to a bacterial type II acyl-carrying protein (ACP) at its 4′-phosphopantetheine cofactor (72). An octanoyl transferase, LipB, conducts the transfer of the octanoyl chain from the ACP to a LCP. The third enzyme in

the pathway, lipoyl synthase (LipA), acts by inserting two sulfur atoms at C-6 and C-8 of the octanoyl backbone, generating the lipoyl cofactor final product (73).

However, in the context of the *M. tuberculosis* pathogen, only the endogenous pathway becomes relevant. This is because the tubercle bacilli have evolved into one-trick ponies when it comes to biosynthesis of the lipoyl cofactor, relying solely upon the actions of ACP, LipB, and LipA rather than LplA (72). Because of this, the *de novo* biosynthesis pathway of lipoic acid becomes an ideal candidate for antibiotic inhibition, inviting further investigation into the nature of the proteins involved.

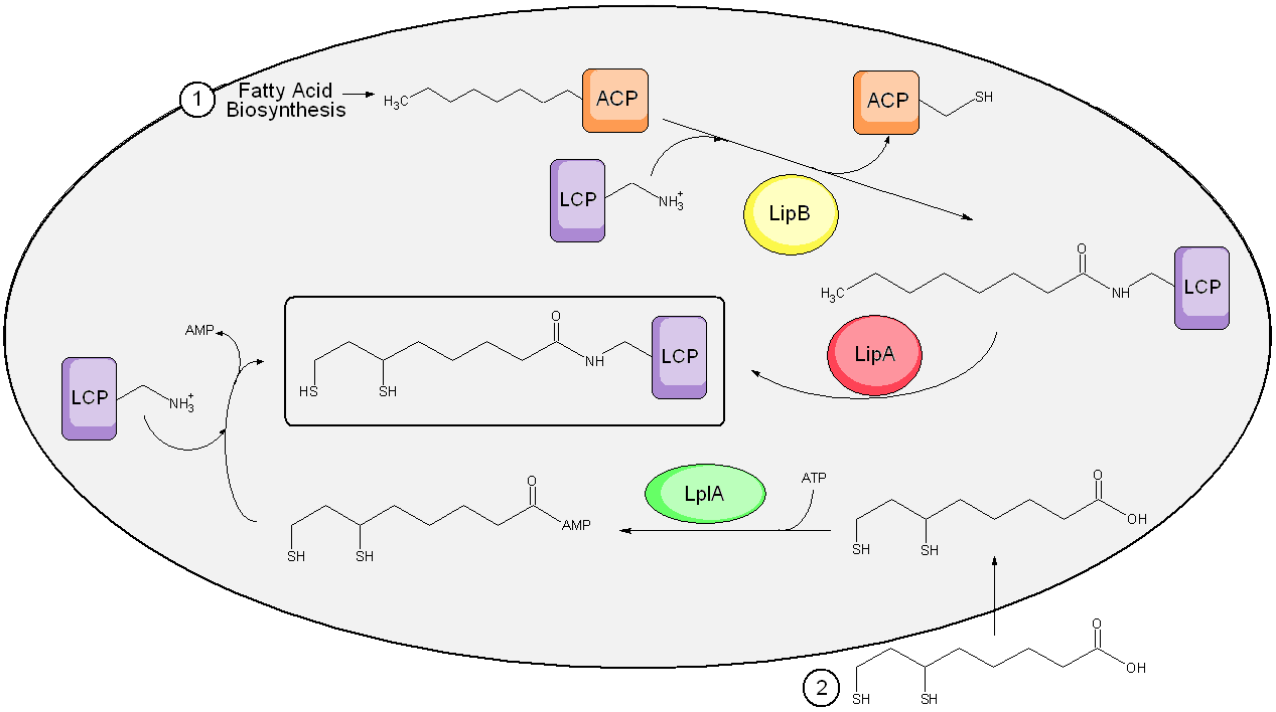


Figure **1-13**: The redundant pathways of lipoyl cofactor synthesis in *E. coli*: the endogenous route also observed in *M. tuberculosis* (1), and the exogenous one that the tuberculosis bacilli lack (2).

## 1.11 Octanoyl Transferase (LipB)

The gene encoding for LipB, *lipB*, was found via experimentation with *E. coli* mutants null for *lplA* (74). It was found that even with a lack of *lplA* gene function, the cells were maintaining growth, as well as function of their large enzyme complexes containing LCPs. The only growth inhibition was observed when there was a second mutation in either the *lipA* or *lipB* genes. The role of LipB in lipoate ligation was confirmed when high expression of *lipB* conferred resistance to selenolipoic acid. This lipoic acid analog inhibits cell growth by binding to protein complexes in the same manner as lipoic acid, but then refusing to undergo reduction as lipoate would to complete the normal complex function (75).

In 2003 researchers Sassetti *et al*. were able to examine LipB in the context of *M. tuberculosis*. Through transposon site hybridization (TraSH), they postulated that *lipB* plays a role necessary for mycobacteria life (76). Supporting this hypothesis, all attempts thus far to grow *lipB M. tuberculosis* mutants have failed. Additionally, via examination of infected lung tissue, expression of LipB has been found to be significantly up-regulated in patients with pulmonary MDR-TB infection (77). Reports released in 2006 by Ma *et al.*, revealed the 3D structure of MtLipB, as well as the discovery that it possesses function as a cysteine/lysine acyltransferase during its catalysis, a feature that sets it apart from LplA (Figure 1-14) (72). When observed as a whole, the implied conclusion of these studies is that LipB, as well as the *de novo* lipoic pathway itself, are promising candidates for antibiotic targeting.

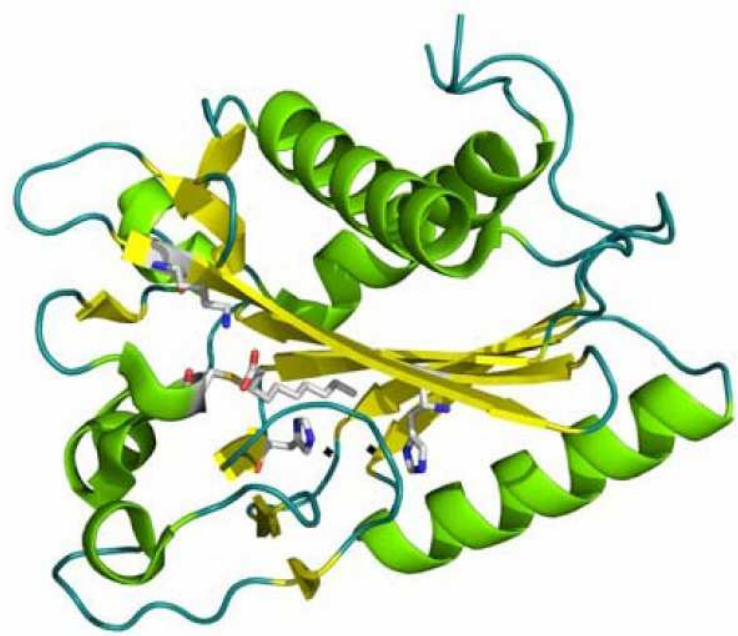

Figure **1-14**: The 3D structure of *M. tuberculosis* octanoyltransferase (LipB) as elucidated by Ma *et al* (72).

## 1.12 Lipoyl Synthase (LipA)

LipA catalyzes the final step of endogenous lipoic acid biosynthesis, inserting sulfur atoms at both the C-6 and the C-8 carbons in the octanoyl group attached to a LCP (Figure 1-15). The *lipA* gene of *E. coli* was first sequenced in 1992 by Ashley *et al*., and later was found to contain 321 amino acids (totaling ~36 kDa in predicted molecular mass) after work in the Cronan laboratory (78,79). Additional research conducted by Cronan and colleagues comprised the first purification of LipA, and confirmed the 36 kDa theoretical molecular mass (79).

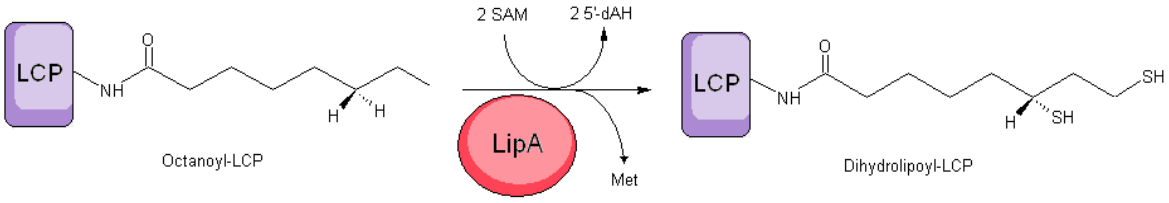


Figure **1-15**: The reaction catalyzed by lipoyl synthase (LipA) at the expense of two S-adenosyl-L-methionine cofactors.

**The iron-sulfur cluster crux of LipA**

In 1999, Marletta *et al*. reported that purification of LipA yielded a reddish-brown protein product, and subsequent metal analysis showed the presence of iron alone. Because LipA was also shown to have 17% sequence homology to biotin synthase (BioB), an enzyme containing a [4Fe-4S] cluster as well as a [2Fe-2S] cluster, it was hypothesized that LipA also harbored an iron-sulfur cluster. Stoichiometric analysis by Marletta and coworkers had indicated the presence of 1.8 mol of iron per protein, and additional sulfide analysis showed the existence of 2.2 mol of sulfide. Though this suggested that the LipA polypeptide included a [2Fe-2S] cluster, UV-visible spectrum analysis and Resonance Raman spectroscopy both indicated presence of a [4Fe-4S] cluster. This was explained using the fact that LipA had purified in both the monomeric and dimeric forms; it was therefore possible that the joining of two [2Fe-2S] cluster-containing LipA monomers created a [4Fe-4S] arrangement upon their joining into a dimer (80).

The Marletta group continued in hot pursuit of the characterization of LipA's iron-sulfur cluster, discovering through gel filtration that LipA occupied mainly the monomeric form. They also reported electron paramagnetic resonance (EPR) spectroscopy results showing that the cluster in non-reduced LipA was of a $[3Fe\text{-}4S]^{1+}$ nature, while reduced was $[4Fe\text{-}4S]^{1+}$ as previously reported. However, further investigation by the Booker and Krebs groups was able to describe the true nature of the LipA iron-sulfur cluster with more conclusive evidence. For the first time Mössbauer spectroscopy joined the lineup of methods used to analyze the enzyme's metal center along with EPR and UV-visible spectroscopies. In this way, they concluded that instead of any of the previously theorized cluster configurations, each LipA monomer contained *two* distinct $[4Fe\text{-}4S]^{2+}$ clusters (73,81).

Confirmation of the presence of an iron-sulfur cluster, combined with further inspection of the *E. coli* LipA peptide sequence in homology studies, suggested that LipA may belong to an emerging group of enzymes, the radical SAM superfamily, all of which contain a [4Fe-4S] cluster lying in a conserved motif (82). All enzymes belonging to the radical SAM superfamily contain a $[4Fe\text{-}4S]^{2+}$ cluster that is ligated by three cysteines in a CXXXCXXC motif ($C_{94}$, $C_{98}$, and $C_{101}$ in *E. coli*). Additionally, lipoyl synthases have been found to possess their very own conserved cysteinyl motif, CXXXXCXXXXXC ($C_{68}$, $C_{73}$, and $C_{79}$ in *E. coli*) (83). Because LipA was thought to contain two [4Fe-4-S] clusters, it was theorized that they were each docked in one of these triple-cysteine motifs. By creating and analyzing *E. coli* that were triple-variants at one motif or the other, it was found that each variant contained one sole iron-sulfur cluster and lacked

lipoyl synthase activity. These results further corroborated the evidence of two [4Fe-4S] clusters belonging to LipA (81).

**LipA's relations: the radical SAM superfamily**

The radical SAM enzyme superfamily is reportedly made up of 2800 metalloproteins, including LipA, biotin synthase (BioB), tyrosine lyase (ThiH), and pyruvate formate-lyase activating enzyme (PFL-AE) (82,84). In addition to their commonality of a conserved CXXXCXXC motif ligated to a $[4Fe\text{-}4S]^{2+/1+}$ cluster, all of the radical SAM superfamily enzymes rely on the generation of a radical from S-adenosyl-L-methionine (SAM, AdoMet) for activity (82). Through studies with electron nuclear double resonance, researchers Walsby *et al*. found that while three of the four iron atoms of the PFL-AE [4Fe-4S] cluster are coordinated via the cysteinyl motif, one has a unique role (84). This singular iron site, they reported, is the agent that anchors the SAM through chelation with the amino and carboxyl regions of the methionine. This anchoring enables the reductive cleavage of $[4Fe\text{-}4S]^{+}$-SAM to $[4Fe\text{-}4S]^{2+}$-Met and a highly reactive 5'-deoxyadenosyl radical (5'dA•) (Figure 1-16) (85). The 5'dA• molecule is capable of initiating radical chemistry through the abstraction of a hydrogen atom from the substrate, which in the case of LipA is the octanoylated-LCP (83).

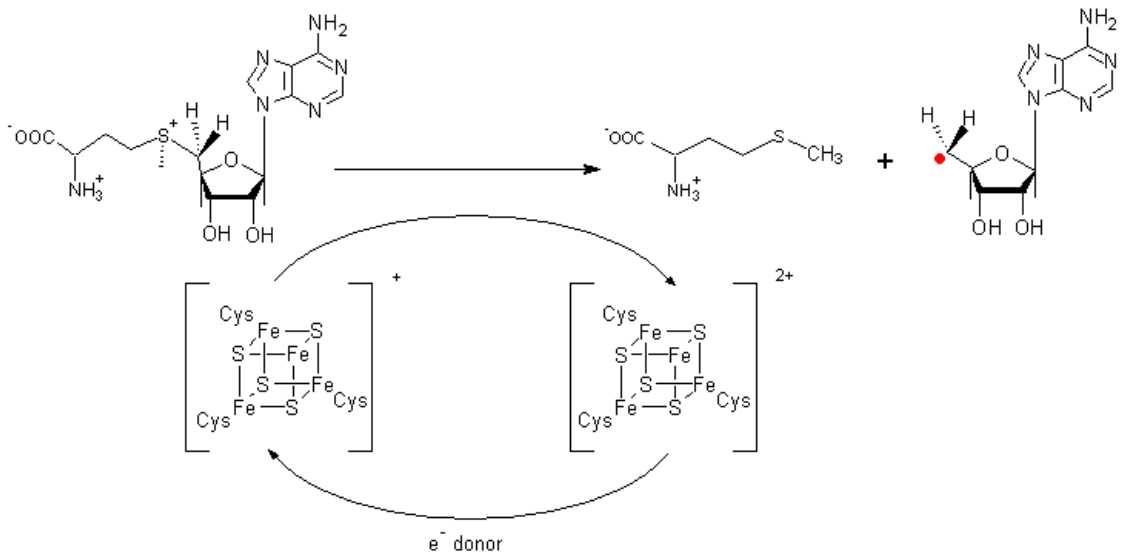


Figure **1-16**: The cleavage of S-adenosyl-L-methionine by a Fe-S cluster during catalysis by an enzyme of the radical SAM enzyme superfamily. The Fe-S cluster donates an electron to the sulfonium of SAM to yield the methionine and 5' deoxyadenosyl radical.

**Mechanistic function of LipA**

Overall, LipA is in charge of introducing two sulfurs into the molecular configuration of the covalently attached octanoyl side arm of a LCP, in a stepwise manner. It is currently thought that this reaction occurs in *E. coli* as follows, as per the results of extensive and continued work in several labs, primarily those of Booker, Cronan, Marletta, and Roach. The 5'dA• radical, generated from the reductive cleavage of SAM as previously discussed, removes the *pro-R* hydrogen atom from carbon 6 in the octanoyl chain (C-6) (83,86). This yields a 5'dA and a C-6 alkyl radical that assails one of the μ-sulfido atoms in the [4Fe-4S] cluster in the tri-cysteine motif at cysteines 68, 73,

and 79, simultaneously reducing an iron atom in the same cluster. Such action results in a monothiolated intermediate species that remains attached to the LCP (83). Then a second 5'dA• radical abstracts a hydrogen at the C-8 position of the octanoyllysine side chain, this time creating a C-8 alkyl radical that, in the same manner, adds to a second bridging μ-sulfido atom of the metal cluster and reduces another iron atom in the process. This stepwise sequence – insertion at C-6 preceding that at C-8 – is indicative of the relative bond strengths of the primary and secondary C-H bonds to be cleaved (87). At this point, two protons have been added to the system, causing the dissociation of the reduced lipoyl cofactor product. The central metallic structure of LipA has lost two sulfurs, and is now spent and thus collapses. This halt of enzymatic activity after just one round of substrate generation explains why *in vitro*, just one turnover event is observed. This working model of activity casts LipA in a double role: as both a catalyst and a substrate.

## 1.13 Conclusion

Elucidation of the nature of the lipoic acid biosynthesis pathway and corresponding characterization of the key enzymes at work has proved a complex, yet fruitful, task. Because the functions of lipoic acid and the lipoyl cofactor within the cell are multifaceted, conserved, and above all, vital, the enzymes that create these compounds make tempting antibiotic targets. If such an antibiotic existed as were capable of targeting an enzyme in the endogenous lipoic acid synthesis pathway in *M. tuberculosis*, theoretically it would be resoundingly effective. The *M. tuberculosis* pathway in question makes an appealing target for yet another reason: though it is

conserved among human cells, *Homo sapiens* is equipped with the backup exogenous pathway run by LplH. Thus imbued, *H. sapiens* cells would be able to maintain the lipoic acid synthesis necessary for their survival whilst tubercle bacilli under experiencing the same pathway inhibition would suffer, and ideally, perish.

It is in this context that the studies herein on *M. tuberculosis* LipA, LipB, and ACP are presented. The genes from all three proteins essential to the *de novo* lipoic acid synthesis mechanism were cloned from genomic *M. tuberculosis* DNA. After successful cloning, the focus was narrowed to just include MtLipA, which was over-expressed heterogeneously in *E. coli* before being purified and characterized to ascertain whether it maintained the structure and function of the *E. coli* analog so thoroughly illuminated already.

# Chapter 2

# Cloning of the Genes Encoding the Protein Trio of the *M. tuberculosis de novo* Lipoic Acid Biosynthesis Pathway and Subsequent Characterization of Lipoyl Synthase

## 2.1 Introduction

The inherent essentiality of the lipoyl cofactor in the metabolism of *M. tuberculosis* makes its biosynthesis a prime target for antibiotic inhibition. Unlike a plethora of other organisms (including humans) that also possess an exogenous synthesis pathway, the tubercle bacilli only have the endogenous enzyme pathway available to them (95). There are three key players in this process: acyl carrier protein (ACP), octanoyltransferase (LipB), and lipoyl synthase (LipA) proteins. The octanoyl fatty acid of an octanoylated ACP (pre-synthesized via the type II fatty acid biosynthetic pathway) is transferred to the lysine residue of a lipoyl-carrier protein (LCP) through action by LipB. LipA then acts on the octanoylated LCP, catalyzing the insertion of sulfur atoms at the sixth and eighth carbons, thus creating the complete lipoyl cofactor. These proteins have all been investigated in their analogous forms existing in *E. coli* bacteria. With the tuberculosis epidemic in mind, we have taken efforts to characterize these three proteins

in *M. tuberculosis*. We undertook this endeavor by first cloning the genes for ACP, LipB, and LipA through polymerase chain reaction (PCR) technique.

Successful cloning allowed for further analysis of one of the three proteins, LipA. Catalyzing the final step in *de novo* lipoic acid synthesis, LipA has garnered attention due to its ability to surmount the energy barrier involved in the process of removing two hydrogen atoms from a fatty acyl chain of saturated carbons without the need for molecular oxygen ($O_2$) to create a suitably potent oxidant. Essential to its enzymatic function is the presence of two iron-sulfur clusters in its structure, ligated to two triple cysteine motifs. The CXXXCXXC motif, as well as LipA's use of S-adenosyl-L-methionine (SAM) as a cofactor, make LipA a member of the Radical SAM Superfamily of enzymes. This motif is located at cysteines 94, 98, and 101 in *Ec*LipA and cysteines 81, 85, and 88 in *Mt*LipA (Figure 2-1), and tethers the Fe-S cluster intimately involved in SAM cleavage. Meanwhile the second triple-cysteine motif, CXXXXCXXXXXC, is located at cysteines 68, 73, and 79 of *Ec*LipA and cysteines 55, 60, and 66 of *Mt*LipA. The Fe-S cluster ligated to this amino acid sequence is believed to function as a sulfur donor during the reaction catalyzed by LipA (89).

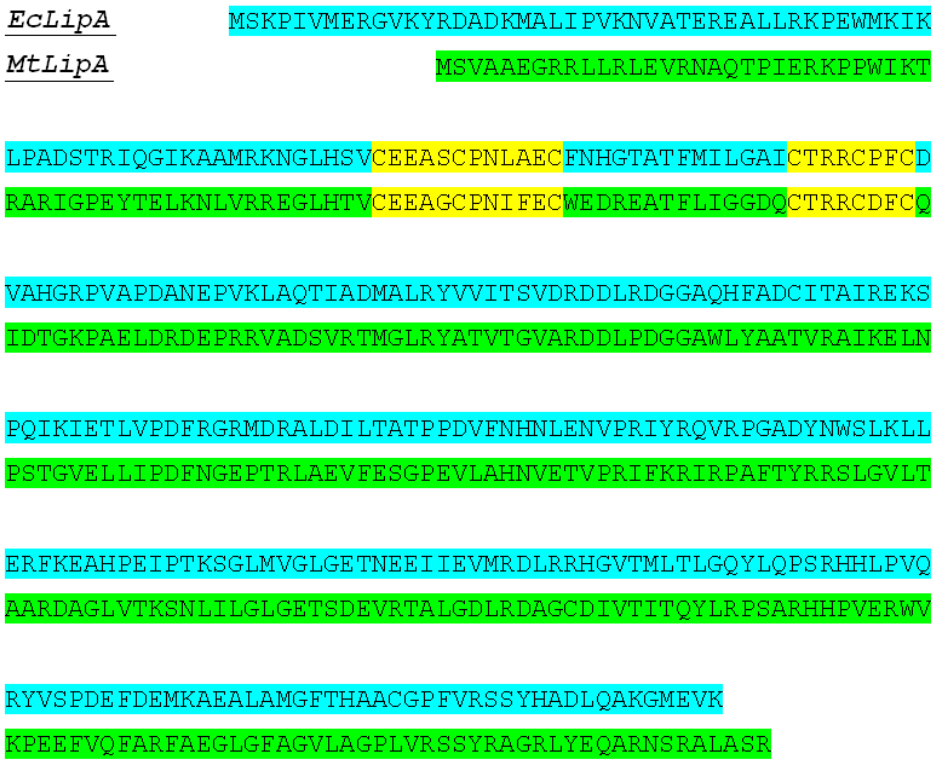


Figure **2-1**: Amino acid sequence alignment of *Ec*LipA (blue, upper line) and *Mt*LipA (green, lower line. Triple cysteines motifs are highlighted in yellow (cysteines 68, 73, and 79, and 94, 98, and 101 for *Ec*LipA, and cysteines 55, 60, and 66, and 81, 85, and 88 for *Mt*LipA). *Mt*LipA contains 311 amino acids as compared to *Ec*LipA's 321 amino acids. Sequence data obtained from the NCBI online database for *E. coli* B21(DE3) and *M. tuberculosis* H37Rv .

Extensive characterization of this superfamily's function has found that they reductively cleave SAM using an $[4Fe\text{-}4S]^{1+/2+}$, creating a 5'-deoxyadenosyl radical (5'dA•) and methionine. Two of the 5'dA• products then act sequentially in the abstraction of a hydrogen atom from the octanoyl moiety attached to a LCP at the C-6 and C-8 positions, allowing for insertion of sulfur atoms at the resulting carbon-centered radicals to create the final lipoyl cofactor product. Previous experimentation has found that LipA action generates 5'dA and lipoyl product in roughly 2:1 stoichiometry, respectively, indicating that two equivalents of SAM are required to produce one lipoyl

product (81). Herein, expression, purification, and characterization of *Mt*LipA were carried out to assess whether the enzyme's structure and function were conserved between *E. coli* and *M. tuberculosis* bacilli.

## 2.2 Materials and Methods

### Materials

The primers used for cloning were provided by Integrated DNA technologies, INC. (Coralville, IA), and ThermoPol polymerase buffer and Vent polymerase were both obtained from New England Biolabs (Ipswich, MA). PfuTurbo buffer and PfuTurbo polymerase are from Stratagene (Cedar Creek, Texas). PET28a vector was purchased from Novagen (Gibbstown, NJ). Kanamycin and ampicillin were provided by IBI Scientific (Pecsto, IA). The Ni-NTA column was from QIAGEN (Valencia, CA), and the $^{57}$Fe was from ISOFLEX USA (San Francisco, CA). pDB1282 plasmid was provided by Dr. Dennis R. Dean, Virginia Tech University. S-adenosyl-$_L$-methionine and lipoyl-H protein were synthesized in the Booker Laboratory according to previously described procedures. All other reagents and chemicals used were reagent grade or higher.

### Cloning of the genes encoding ACP, LipB, and LipA

Each gene was cloned from *Mycobacterium tuberculosis* genomic DNA (strain H37Rv) with the use of primers acpforNdeI and acprevEcoRI for *acp*, lipbforNdeI and

lipbrevEcoRI for *lipb*, and lipaforNdeI and liparevEcoRI for *lipA*, with sequences shown in Table 2-1. The first PCR reactions for each gene were conducted in duplicate, and each contained 2 μL of 100 ng/μL *M. tuberculosis* genomic DNA, 1 μL of each of the corresponding 20 μM forward and reverse primer stocks, 5 μL of a 2.5 mM dNTP mixture, 5 μL 10X ThermoPol polymerase buffer, 1 μL Vent polymerase, and 35 μL sterilized $dH_2O$ for a total reaction mixture volume of 50 μL. To the surfaces of all six mixtures, 35 μL mineral oil was added, and the tubes centrifuged. The PCR reaction was conducted using a Stratagene Robocycler Gradient 40 machine. The samples were incubated at 95 ˚C for 9 minutes, after which 35 cycles of 1 min at 95˚C (denaturing temperature), 1 min at 55 ˚C (annealing temperature), and 2.5 minutes at 72 ˚C (elongation temperature) were performed. Following this the PCR tubes were incubated at 72 ˚C for another 10 minutes. All six PCR products were visualized using a 1.5% agarose gel stained with ethidium bromide (EtBr) to determine whether the bands indicated products of the correct length, in nucleotides (nt). There were no distinct bands observed of the expected sizes, for any of the three genes. Therefore a second PCR procedure was performed, identical to the first except with an annealing temperature of 60 ˚C. The gel bands corresponding to *acp* were the correct size, and were therefore removed using a razor, extracted from the agarose gel using a Qiagen Gel Extraction Kit, and stored to await the successful PCR of *lipb* and *lipa*.

A third, fourth, and fifth PCR reactions were carried out, the same as before except with annealing temperatures of 60 ˚C, 50 ˚C, and 45 ˚C, respectively. None were met with success, so another duplicate PCR reaction mixture was conducted for both *lipb* and *lipa*, containing 4 μL 66 ng/ μL *M. tuberculosis* genomic DNA, 2 μL of each gene's

corresponding 20 μM forward and reverse primers, 5 μL 2.5 mM dNTP mixture, 5 μL 10X PfuTurbo polymerase buffer, 1 μL PfuTurbo polymerase, and 31 μL sterilized $dH_2O$ to create a total reaction volume of 50 μL, to which 35 μL mineral oil was added. The resulting four samples underwent PCR as previously described in the first PCR attempt, with an annealing temperature of 55 ˚C. When visualized as before, these PCR products met the expected nt lengths and were excised from the gel, and extracted using a Qiagen Gel Extraction Kit.

| **Primer** | **Sequence** | **Purpose** |
|---|---|---|
| acpforNdeI | CGC GGC GTC CAT ATG AGT GTC GCT GCC GAG GGC CGG CGC C | Forward primer for cloning *acp* |
| acprevEcoRI | CGC GGC GTC GAA TTC CTA GCG GGA TGC CAA GGC CCG TGA GTT | Reverse primer for cloning *acp* |
| lipbforNdeI | CGC GGC GTC CAT ATG ACG GGT TCT ATC CGG TCG AAG CTG TCC | Forward primer for cloning *lipb* |
| lipbrevEcoRI | CGC GGC GTC GAA TTC TCA TAA CGG CGA TGG TAC GGC GTG TGA GGG | Reverse primer for cloning *lipb* |
| lipaforNdeI | CGC GGC GTC CAT ATG CCT GTC ACT CAG GAA GAA ATC ATT GCC | Forward primer for cloning *lipa* |
| liparevEcoRI | CGC GGC GTC GAA TTC TCA CTT GGA CTC GGC CTC AAG CCT CGC C | Reverse primer for cloning *lipa* |

Table **2-1**: Primer sequences used in the cloning of *M. tuberculosis* acyl carrier protein, octanoyltransferase, and lipoyl synthase. Restriction enzyme sites are underlined.

The PCR products of all three genes and a pET28a vector were digested in four separate reactions with the restriction enzymes *Nde*I and *Eco*RI. The digests contained 43 μL *acp*, *lipb*, or *lipa* PCR products, 5 μL 10X *Eco*RI buffer, 1 μL *Eco*RI, and 1 μL *Nde*I, for a total reaction volume of 50 μL. The fourth digest contained 2 μg pET28a, 1.5 μL *Eco*RI buffer, 1 μL *Eco*RI, 1 μL *Nde*I, and 3 μL sterilized $dH_2O$ for a total reaction volume of 15 μL. All restriction digests were incubated overnight at 37 ˚C, and then

visualized under UV light on a 1% agarose gel with EtBr staining. Each fragment was excised, and extracted from the gel using a Qiagen Gel Extraction Kit, after which their concentrations were determined using a Biophotometer 6131 machine (V1.35).

The digested PCR gene products were ligated into the digested pET28a vector in reaction mixtures containing the following components: 100 ng pET28a, 300 ng of the gene to be inserted, 1.5 µL T4 DNA ligase buffer, 1 µL T4 DNA ligase, and enough sterilized $dH_2O$ to bring the total reaction volume up to 15 µL. The ligation mixtures were incubated at 4 ˚C overnight. Through the cloning of the gene inserts into the *Nde*I site of the pET28a vector, a hexahistidine tag could be incorporated at the N-terminus of the encoded ACP, LipB, and LipA proteins. The ligation mixtures were then transformed into *E. coli* dh5α cells on LB/kanamycin agar plates. Restriction analysis with *Nde*I and *Eco*RI (and visualization via gel electrophoresis) and subsequent DNA sequencing at the Penn State DNA Sequencing Facility verified that each of the three resulting plasmids contained the correct insert. Each plasmid was then separately purified using a Qiagen Plasmid Midi Prep Kit, and the samples stored in glycerol solution.

**Expression of LipA**

BL-21 DE3 *E. Coli* cells were co-transformed with an 938 ng/µL $Amp^R$ plasmid pDB1282 encoding the necessary proteins for iron-sulfur cluster assembly, and a 658 ng/µL plasmid containing a hexahistidine-tagged previously cloned *M. tuberculosis lipA* gene in a $Kan^R$ pET28a vector. This was done on a 1% agar LB plate containing 50 µg/mL kanamycin and 100 µg/mL ampicillin. Two of the resulting colonies (designated

#1 and #4) were each used to inoculate starter cultures of LB media, 50 µg/mL kanamycin and 100 µg/mL ampicillin, and incubated in a shaker overnight at 37 ˚C and 250 rpm. Then 1 mL of each starter culture was inoculated into 100 mL LB/kanamycin/ampicillin, and the cultures grown until they reached an $OD_{600}$ of about 0.3. At this point a 1 mL sample from each flask was removed, centrifuged for 2 minutes at 14,000 rpm, the supernatant removed, and the resulting pellets set aside on ice for future SDS-PAGE gel analysis. To the two flasks, liquid L-(+)-arabinose was added to a final concentration of 0.2% w/v, and the cells were allowed to grow until an $OD_{600}$ of approximately 0.6. A 1 mL sample was removed from each, and prepared as before. In order to induce expression of the desired protein in the growing cultures, 50 µL 0.1 M FeCl3 (for a final concentration of 50 µM) and 200 µL 0.1 M ITPG (for a final concentration of 200 µM) were added to each culture flask. Each hour for 4 hours, $OD_{600}$ was measured, and a sample taken from each flask and prepared as before. Then three 1.5 mL 25% glycerol aliquots were made of each culture, and the aliquots stored at –80 ˚C. The 1 mL samples taken throughout were each mixed with 50 µL $dH_2O$ and 50 µL 2X SDS buffer, and incubated in boiling water before being run and visualized on a SDS-PAGE polyacrylamide gel.

In the second expression study, two 4 mL starter cultures of M-9 minimal media were each inoculated with cells from the same two colonies as the first study, and grown overnight. The next day, 1 mL from each starter culture was transferred to a flask containing 100 mL M-9 minimal media, 50 µg/mL kanamycin and 100 µg/mL ampicillin. When $OD_{600}$ reached 0.3, a 1 mL sample was removed from each flask and prepared as before for later SDS-PAGE analysis, and liquid L-(+)-arabinose was added to a final

concentration of 0.2%. At $OD_{600}$ = 0.6, a 1 mL sample was removed and prepared as before, and $FeCl_3$ and IPTG were added to final concentrations of 50 μM and 200 μM, respectively. The cultures were then allowed to continue growth overnight in the shaker (18 ˚C and 250 rpm). The next day a third sample was removed and prepared, and the three samples taken for each culture (six total) were run and visualized on a SDS polyacrylamide gel.

A third and final expression study was run using cells taken only from colony #4. This colony was used to inoculate a starter culture of 200 mL M-9 minimal media containing 50 μg/mL kanamycin and 100 μg/mL ampicillin, and the culture was grown for approximately 24 hours in the shaker as before. Then 16 L (4 x 4 L) M-9 minimal media (containing 50 μg/mL kanamycin and 100 μg/mL ampicillin) was inoculated with 400 μL each of the starter culture and incubated at 37 ˚C while shaking at 180 rpm. Once $OD_{600}$ reached 0.3, a 1 mL SDS sample was removed from each of the four flasks and prepared as before, and then liquid L-(+)-arabinose was added to a 0.2% final concentration. At $OD_{600}$ = 0.6, 1 mL samples were taken, and the flasks were removed from the incubator and chilled on ice until cool. Then FeCl3 and IPTG were added to each flask to final concentrations of 50 μM and 200 μM, respectively, and the flasks left to incubate in the shaker for an additional 21 hours at 18 ˚C and 180 rpm. At this point, a last 1 mL sample was taken from each flask, and the three samples collected for each flask were run on two SDS polyacrylamide gels at 40 mA. Meanwhile, the cells from the 4L cultures were harvested via centrifugation at 4 ˚C and 10,000 x g, before being frozen and stored in liquid nitrogen.

**Initial Purification and Reconstitution of LipA**

With the exception of centrifugation, all of the following purification steps were conducted within the confines of a Coy anaerobic chamber (Coy Laboratories; Grass Lake, MI) and on ice, unless otherwise stated. The chamber atmosphere was maintained at 95% nitrogen / 5% hydrogen, and ≤ 1 ppm oxygen with the help of Palladium catalysts. Water used within the chamber was previously deoxygenated by boiling 6 L $dH_2O$ to 4 L, and stirring within the chamber for 24 hours. Any autoclavable plastics were autoclaved, brought into while the chamber while still hot, and allowed to equilibrate for 24 hours. Plastics that could not be autoclaved were allowed to equilibrate within the chamber for a minimum of 1 week before use.

Four buffers were prepared prior to LipA purification: lysis buffer (100 mM Hepes pH 7.5, 300 mM KCl, 20 mM imidazole, 10 mM β-mercaptoethanol (BME), 1 mM L-cysteine, 0.1 mM pyridoxal-5-phosphate (PLP), 5 mM $MgCl_2$, 5 mM ATP, and $H_2O$ to a total volume of 200 mL), wash buffer (100 mM Hepes pH 7.5, 300 mM KCl, 40 mM imidazole, 10 mM BME, 20% glycerol, and $H_2O$ to a total volume of 200 mL), elution buffer (100 mM Hepes pH 7.5, 300 mM KCl, 250 mM imidazole, 10 mM BME, 20% glycerol, and $H_2O$ to a total volume of 250 mL), and gel filtration buffer (50 mM Hepes pH 7.5, 300 mM KCl, 1 mM dithiothreitol (DTT), 20% glycerol, and $H_2O$ to a total volume of 1 L). All four buffers were cooled on ice before being used at any point in the experiment. A Ni-NTA column (2.5 x 6 cm) for affinity chromatography was constructed with about 35 mL resin, and equilibrated with cold lysis buffer prior to use.

The frozen cells harvested from the third expression study were suspended in 100 mL lysis buffer, and 1 mg/mL lysozyme was added to the mixture and left to stir for 30 minutes at room temperature. Using a sonicator, the cells were lysed in five 1-minute bursts, and the resulting lysate was aliquoted into four centrifuge tubes, which were then taped to maintain the integrity of the cell mixture's anaerobic environment. The crude lysate was centrifuged at 50,000 x g and 4 ˚C for 1-1.5 hours, before being applied by gravity to the top of the prepared column. Then 150-200 mL wash buffer was run through the column. Using the prepared elution buffer, LipA was eluted from the column into a single, dark brown fraction. The entirety of this fraction was concentrated in an Amicon (Millipore) stirred cell with a YM-10 membrane (pore size 10 kDa), and then loaded on to a G-25 gel filtration column (pre-equilibrated with cold gel filtration buffer) where it was eluted with gel filtration buffer. After elution, the protein was once again concentrated using the Amicon stirred cell, before freezing and storing it in liquid nitrogen. The concentration of the LipA protein product was determined using the Bradford method, employing a correction factor of 1.47 and standards made with 1 mg/mL bovine serum albumin (BSA). This is the same correction factor used for *E. coli* LipA, and it is necessary because when BSA is used as a standard as the Bradford method overestimates sample protein concentration (81,89). Success of the purification procedure was verified using SDS-PAGE.

A portion of the protein product was then reconstituted to obtain LipA with fully replenished Fe-S clusters that may have been depleted or otherwise lessened during the purification process. The reconstitution procedure was carried out anaerobically, on ice, in a final reconstitution mixture volume of 20 mL. To the desired volume of purified

LipA, DTT was gradually added over a time period of 1-2 hours to a final concentration of 5 mM. Next, $FeCl_3$•$6H_2O$ was added in a similar manner over the course of 30 minutes to a final concentration of 800 μM, and 160 μL $Na_2S$ was added during the following 2 hours to a final concentration of 800 μM. The entire sample was then left on ice overnight, before being concentrated in an Amicon, centrifuged at 14,000 rpm, run through a G-25 gel filtration column with the leftover gel filtration buffer from the purification, and collected in a single, dark brown fraction. This protein elution was then concentrated once more using the Amicon. The resulting reconstituted (RCN) protein sample was then subjected to the same Bradford analysis procedure as the remaining as-isolated (AI) protein.

**Initial Characterization of LipA**

**Fe-S Analysis**

Dilutions of the protein products (1 in 50) were tested with UV-visible spectroscopy to estimate the amounts of Fe-S cluster present in each. The ratio of the peak height at 280 nm / peak height at 410 nm was calculated, a value usually measuring between 2.5 and 3 for *E.coli* LipA protein (89).

Iron analysis was conducted for both RCN and AI protein. Protein samples were analyzed in quadruplicate, in 300 μL, 4 μM dilutions created using gel filtration buffer. The nine standards used were created using 100 μM Fe standard solution (Claritas PPT iron standard, 2% $HNO_3$ solution, $dH_2O$). To each 300 μL sample or standard, 300 μL

Reagent A (1.35 g SDS, 450 µL saturated Fe-free NaOAc, 30 mL $dH_2O$) and 300 µL Reagent B (270 mg ascorbic acid, 9 mg sodium meta-bisulfate, 400 µL saturated Fe-free NaOAc, 5.6 mL $dH_2O$) were added and then mixed and incubated in a water bath at 37 °C for 15 minutes. Fifteen µL Reagent C (18 mg ferene, 1 mL $dH_2O$) was added to each sample/standard, and they were centrifuged for at 14,000 rpm (at least 5 minutes) until just before reading their absorbances at 595 nm.

Both RCN and AI protein then underwent sulfide analysis (all steps conducted anaerobically). Protein samples were run in quadruplicate (4x100 µL) 12 µM dilutions in $dH_2O$. Sulfide standards were created using dilutions of 200 µM $Na_2S$ and $dH_2O$. To each 100 µL standard and sample, 300 µL 1% zinc acetate, and then 15 µL 12% NaOH were added, mixed, and allowed to stand for 1-2 hours. Each mixture was then underlaid with 75 µL 0.1% DMPD solution, and 2 µL 23 mM $FeCl_3$ solution added, and each solution mixed. All solutions were then centrifuged at 14,000 rpm for 15 minutes, and 400 µL of the resulting supernatant of each was brought to 1 mL with 2 mM pH 8 EPPS buffer. Solutions stood for 30 minutes at room temperature, before their absorbances were measured at 670 nm.

**Activity assay with octanoyl-peptide**

The protein samples were then assayed to ensure the expected enzymatic activity was present, as well as to compare the relative activity levels of the AI and RCN isolates. The assay mixtures contained 50 mM pH 7.5 HEPES, 2 mM dithionite, 1 mM tryptophan

internal standard, 500 μM octanoyl-peptide, and 200 μM AI protein brought to 1.1 mL with $dH_2O$ and incubated at 37 °C for 3 minutes. To initiate the reaction, 0.7 mM SAM cofactor was added and 100 μL and 25 μL aliquots removed at fixed time points (0, 2, 5, 10, 15, 20, 25, and 30 minutes) and quenched in Eppendorf tubes containing 100 μL and 25 μL of 100 mM $H_2SO_4$ (respectively). A control mixture was run simultaneously without the addition of SAM, from which 100 μL and 25 μL aliquots were removed after 30 minutes and quenched in 100 mM $H_2SO_4$.

The 100 μL/100 μL samples were then analyzed for enzyme activity spectrophotometrically. After centrifuging for 5 minutes at 14,000 x g, 100 μL of the resulting supernatant was removed, and the rest was discarded. To this supernatant was added an assay mixture of 50 mM HEPES pH 7.5, 8 mM TCEP, 2 mM $NAD^+$, and $dH_2O$ in a final volume of 1100 μL. Right before reading their absorbance at 340 nm using the Cary WinUV Kinetics program, 5 μL $H_2$LipDH was added and the samples mixed by inversion. Sample readings were analyzed via comparison to Lipoyl-H protein standards. Meanwhile, using the previously described HPLC analysis method, the 25 μL/25 μL samples were assessed to quantify the amount of 5'-dA produced.

This assay procedure was repeated using 20 μM flavodoxin, 5 μM flavodoxin reductase, 1 mM NADPH, and 1 mM DTT in place of the 2 mM dithionite previously used. In doing so it was possible to assess whether assaying with a chemical (dithionite) or biological (flavodoxin) reductant produced better results in terms of enzyme activity. Based on the lackluster results of the assay with flavodoxin, only dithionite was used in this capacity for the remainder of experimentation.

**Second Purification and Characterization of LipA**

Following the first purification and analysis procedures, it became necessary to obtain additional LipA product for further study. Cells from the 25% glycerol pET28a *Mt*LipA pDB1282 BL-21 DE3 stock previously stored at –80 ˚C were once again grown on a 1% agar LB/Kan/Amp plate, before their inoculation into a M9 salts minimal media starter culture. From this point, the scale up for cell harvesting was repeated as before, with the exception that in the place of $FeCl_3$, the $^{57}Fe$ isotope (prepared by Kyung-Hoon Lee) was used during expression to allow for future Mössbauer spectroscopy. The resulting cells were harvested as before, and subsequent purification conducted following the same procedure. A portion of the resulting protein product was reconstituted, again using $^{57}Fe$ (to a final concentration of 800 μM in the reconstitution mixture) in the place of $FeCl_3$. Both the AI and RCN protein samples obtained (hereby referred to as $^{57}$AI and $^{57}$RCN) were analyzed via the Bradford method to determine their respective concentrations, and both underwent UV-visible spectroscopy analysis to approximate the quantity of Fe-S cluster present. Additionally, both proteins underwent iron and sulfide analysis, as well as an octanoyl-H activity assay, as conducted previously with the initial protein samples.

**Preparation of samples for Mössbauer Spectroscopy**

Samples were prepared for both $^{57}$AI and $^{57}$RCN protein samples in the Coy anaerobic chamber. To obtain an iron concentration of 2-2.5 mM in each 250 μL Mössbauer sample, $^{57}$AI protein was diluted to 290 μM in chilled gel filtration buffer

(leftover from the second purification procedure), and $^{57}$RCN protein to 255 μM. Each protein dilution was transferred into its own plastic cup and frozen in liquid nitrogen until its analysis.

**Electron Paramagnetic Spectroscopy (EPR)**

All EPR samples were created in the Coy anaerobic chamber. To accompany the preceding Mössbauer samples, $^{57}$AI and $^{57}$RCN proteins were each diluted to 290 μM and 255 μM (respectively) in 250 μL with gel filtration buffer, before being transferred to EPR tubes. The tubes were submerged in liquid nitrogen-cooled isopentane before being frozen in liquid nitrogen and stored until their EPR analysis.

Because of its performance in the previous octanoyl-H activity assay, $^{57}$AI protein was selected for additional analysis. The first 250 μL EPR sample contained 200 μM $^{57}$AI protein, 700 μM SAM, 8 mM dithionite, and $dH_2O$. The next six samples were collected as time points from a 1750 μL reaction mixture containing 200 μM $^{57}$AI protein, 50 mM HEPES pH 7.5, 8 mM dithionite, 500 μM octanoyl-peptide, and $dH_2O$, initiated by the addition of 0.7 μM SAM. Aliquots of 250 μL were removed at 0, 3, 6, 10, 30, and 60 minutes and used to create EPR samples as described above. All samples were analyzed with an ESP 300 spectrometer.

Each protein sample was analyzed through EPR spectroscopy at a temperature of 13 K, power of 5.02 mW, gain of $2e^4$, time constant of 163.84 milliseconds, conversion time of 81.92 milliseconds, and modulation amplitude of 10.2 Gauss. All samples, including the blank (50 mM HEPES, pH 7.5) were read at two distinct settings: center

field of 3480 Gauss and sweep width of 2000 Gauss, and center field of 2600 Gauss and sweep width of 5000 Gauss. Those samples containing quenched reaction mixtures included the conditions necessary for reaction turnover, as well as appropriate substrate analogs.

## 2.3 Results

### UV-visible spectra and SDS-PAGE

The initial 16 L expression of LipA yielded 37 g of cell paste, from which 4.5 mL of AI LipA protein was obtained. The $A_{280}/A_{410}$ ratio obtained through UV-visible spectroscopy reported a value of 3.2, and the concentration as reported by the Bradford method was 656 μM protein, giving a total of 110 mg protein collected (Figure 2-2). LipA reconstitution utilized 3 mL of the 4.5 mL AI protein, yielding 3.7 mL RCN protein with a measured concentration of 410 μM and 56 total mg. The UV-visible $A_{280}/A_{410}$ for RCN protein was found to be 2.2. In the second expression scale-up of LipA, 35 g of cells were harvested, and subsequent purification yielded 3.5 mL 1657 μM $^{57}$AI protein (225 mg protein) with an $A_{280}/A_{410}$ of 2.9. LipA reconstitution produced 1.8 mL 644 μM $^{57}$RCN protein (38 mg total protein) with an $A_{280}/A_{410}$ of 2.5. The SDS-PAGE gels run with samples taken throughout the purification procedures confirmed that the AI and $^{57}$AI isolates obtained were sufficiently pure (≥98%) for continued experimentation (Figure 2-3).

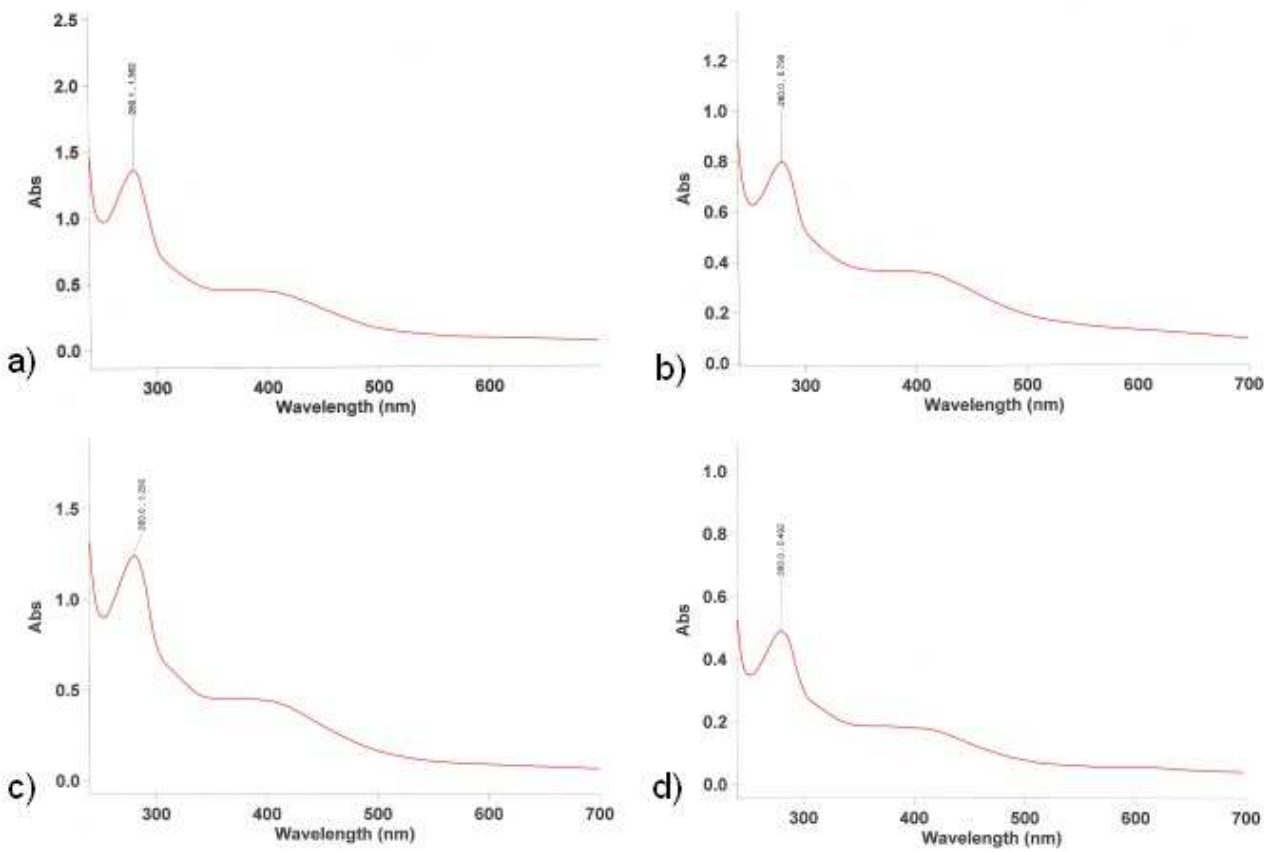


Figure **2-2:** UV/visible spectroscopy results for 1/50 diluted AI (a), 1/50 diluted RCN (b), 1/100 diluted $^{57}$AI (c), and 1/100 diluted $^{57}$RCN protein samples (d). Each was analyzed at 240-700 nm.

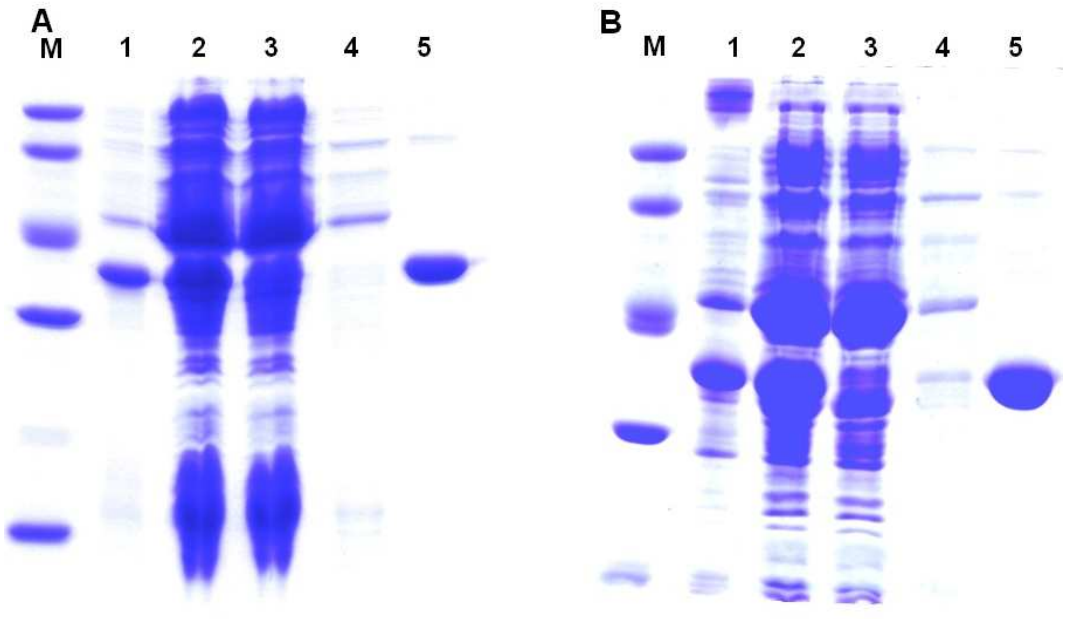


Figure **2-3**: SDS-PAGE gel analysis of purification of AI LipA (A) and $^{57}$AI LipA (B). The lanes depicted contain low molecular weight markers (M), crude pellet (1), crude supernatant (2), load flow-through (3), wash flow-through (4), and final purified protein product (5).

**Fe-S analysis of *Mt*LipA**

Fe and S analysis results for all four protein batches are listed below in Table 2-2. In the case of the AI and RCN protein samples, analysis showed ~ 7-11 Fe and ~ 11-13 S per LipA monomer. Meanwhile the $^{57}$AI and $^{57}$RCN samples reported lower values: ~ 7-8 Fe and ~ 5-8 S per monomer, numbers that are in accordance with previous work on *E. coli* LipA in the Booker Laboratory by Master's student Elizabeth Billgren (89). These numbers are within the expected range since a LipA monomer containing two intact [4Fe-4S] clusters would have 8 equivalents of both Fe and S.

| Purification | Protein Sample | Average μM Fe/Protein Observed | Average μM S/Protein Observed |
|---|---|---|---|
| 1 | AI | 7.4 | 11.0 |
| | RCN | 10.4 | 12.4 |
| 2 | $^{57}$AI | 7.0 | 5.1 |
| | $^{57}$RCN | 7.9 | 8.2 |

Table **2-2**: Iron and sulfide analysis results for both batches of purified as-isolated and reconstituted proteins.

**Octanoyl-peptide activity assays**

An assay with octanoyl-peptide was conducted to assess the activity of the AI and RCN LipA proteins from both purification procedures. Each LipA protein was incubated with substrate (octanoyl-peptide), SAM, chemical reductant (dithionite), tryptophan internal standard and HEPES reaction buffer. Aliquots were removed as the reaction progressed to be analyzed for the presence of lipoyl H-protein, the final product and thus an indicator of protein activity. Both sets of protein showed higher activity in the AI samples versus the RCN, though in the $^{57}$Fe batches only a slight difference in activity was observed (Figure 2-4). The AI, $^{57}$AI, and $^{57}$RCN reaction mixtures afforded 90-100 μM Lipoyl-H by the 30-minute end point, a concentration measuring about half that of the starting 200 μM LipA protein. This indicates that for every two LipA proteins, one Lipoyl-H was generated. On the other hand, when the AI and RCN samples were run in an identical activity assay, but with flavodoxin as the reductant, the decrease in LipA activity was so drastic that barely any activity was observed at all (Figure 2-5).

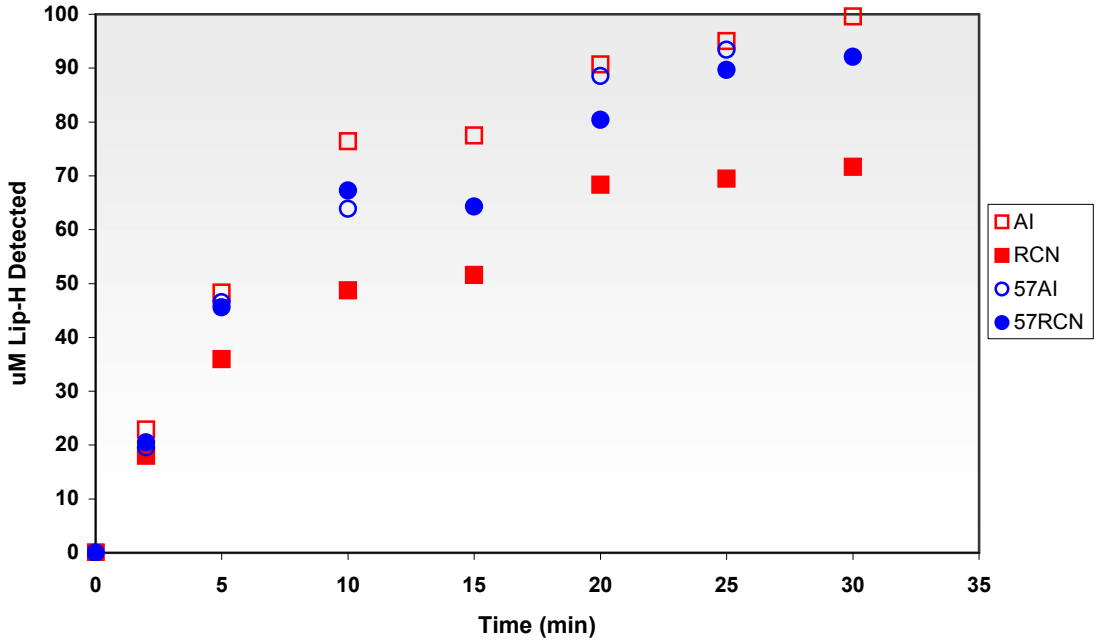


Figure **2-4**: LipA enzyme activity as determined by four different assays measuring accumulation of lipoyl-H in the presence of SAM, octanoyl-peptide, and dithionite reductant. Eight time points were collected for each sample, with the exception of $^{57}$AI, for which there wasn't enough material for readings at 15 minutes and 30 minutes.

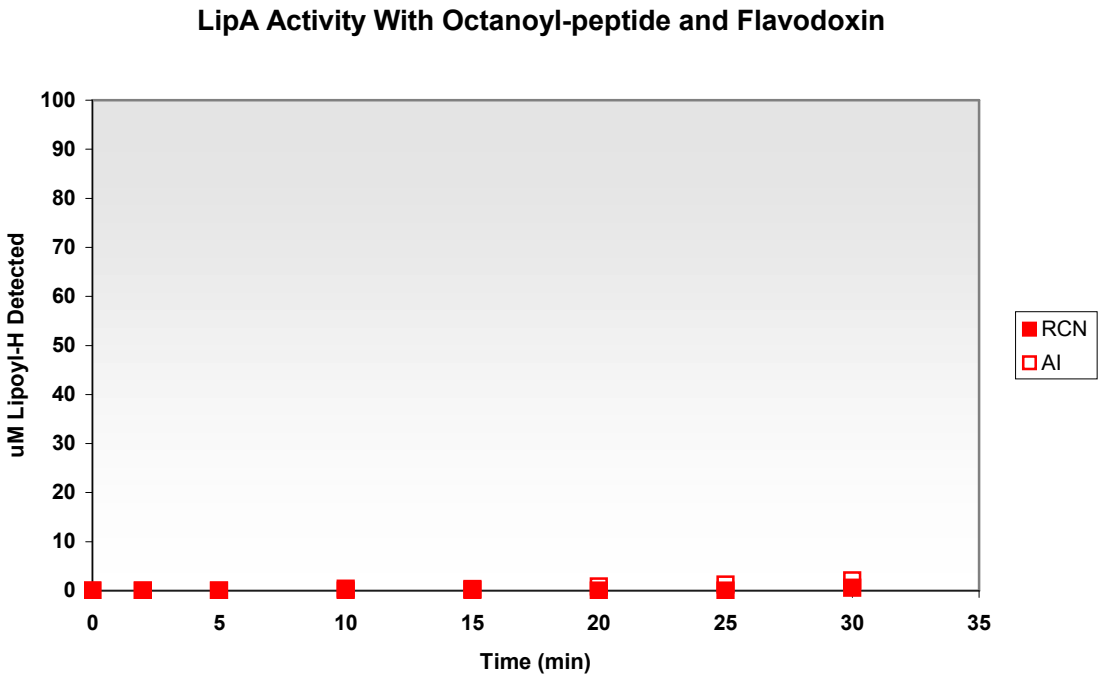


Figure **2-5**: LipA enzyme activity for AI and RCN samples in the presence of octanoyl-peptide, SAM, and flavodoxin reductant.

Because 5'dA is a product indicative of proper LipA function, measuring the 5'dA content of the activity assay time points collected directly reflects enzyme activity. This was done using HPLC technology. By the close of the assay with dithionite, AI LipA had produced ~350 µM 5'dA, and RCN LipA ~250 µM 5'dA. This data indicates that more than one product was generated, on average, per LipA enzyme. Specifically for AI protein, there were approximately 1.75 units of 5'dA produced/protein. Once again the activity in the presence of flavodoxin rather than dithionite was negligible, and the AI protein isolate was observed to have more activity than the RCN (Figure 2-6).

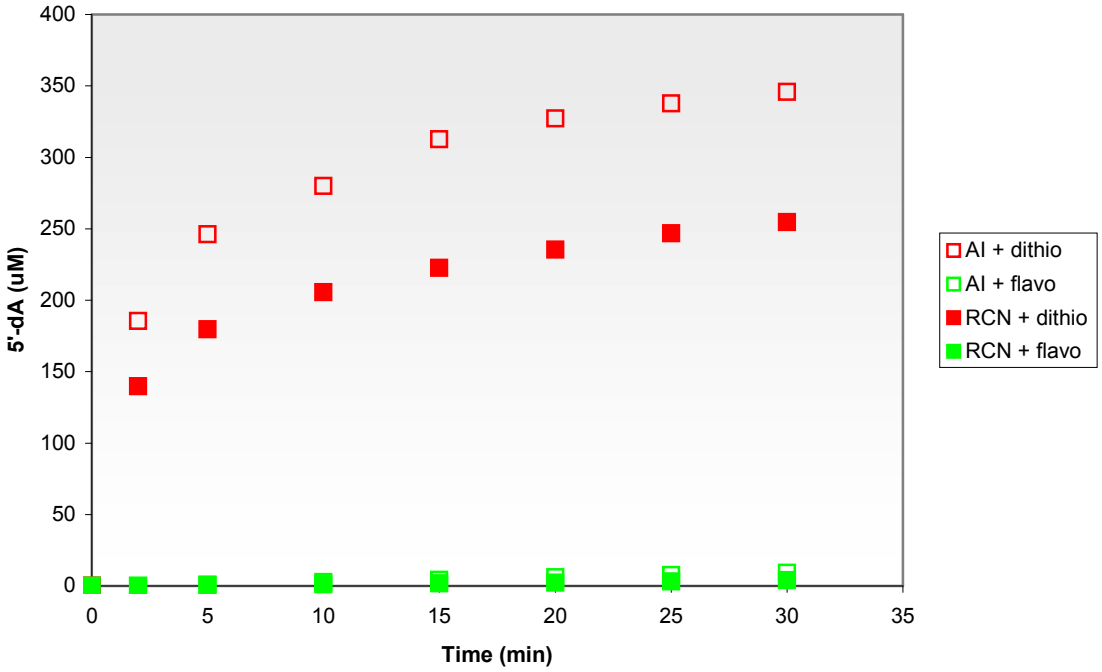


Figure **2-6**: AI and RCN LipA enzyme activity, measured in terms of amount 5'dA produced, in the presence of either dithionite or flavodoxin reductants, octanoyl-peptide, and SAM. Data obtained via HPLC.

## Mössbauer and EPR spectra for $^{57}$AI and $^{57}$RCN *Mt*LipA

Mössbauer and EPR spectroscopy were employed to better ascertain the nature of *Mt*LipA's iron-sulfur clusters. Both $^{57}$AI and $^{57}$RCN proteins yielded 4.2-K/53-mT Mössbauer spectra dominated by a quadrupole doublet (Figure 2-7). It is possible to analyze these spectral results through comparison with parameters typical of $[4Fe\text{-}4S]^{2+}$ clusters: one broad quadrupole doublet with a quadrupole splitting parameter ($\Delta E_Q$) of 1.14 mm/s and isomer shift ($\delta$) of 0.45 mm/s. In the case of $^{57}$AI LipA, which has a total of ~7.0 Fe/polypeptide, such a quadrupole doublet accounts for 96% of total Fe (solid

line in Figure 2-7A). The spectrum exhibited here by AI *Mt*LipA is almost identical to those previously published for *E. coli* LipA (81). Additionally, spectra obtained over a wider range of Doppler velocities (data not shown) indicate that the protein sample did not contain a significant amount of Fe species (<5% of total Fe) exhibiting a magnetically split subspectrum. The corresponding EPR spectrum for $^{57}$AI *Mt*LipA reveals a minute amount of $[3Fe\text{-}4S]^{+}$ cluster presence (~6 μM), corresponding to ~0.4% of the total amount of Fe present in the protein sample (Figure 2-8). A Mössbauer spectrum for a $[3Fe\text{-}4S]^{+}$ cluster is a superposition of three magnetically split subspectra, as a result of the three discrete Fe sites (90). In this case the ~0.4% contribution of the $[3Fe\text{-}4S]^{+}$ clusters is undetectable via Mössbauer since the subspectra for different $[3Fe\text{-}4S]^{+}$ clusters are relatively broad and similar to one-another (91). Furthermore, the appearance of $[3Fe\text{-}4S]^{+}$ cluster presence disappears upon reduction of the sample with dithionite, and though the resulting signal is noisy, it is consistent with $[4Fe\text{-}4S]^{2+}$ clusters (Figure 2-9). Together with the Fe-S quantification results indicating 7.0 Fe per protein, these spectral results indicate a stoichiometry of 1.7 [4Fe-4S] clusters per AI *Mt*LipA polypeptide.

The Mössbauer spectrum resulting from the $^{57}$RCN sample (~7.9 total Fe) was identical to that of the $^{57}$AI sample, allowing for experimental uncertainty. The simulation representing the parameters for the typical $[4Fe\text{-}4S]^{2+}$ cluster accounts for 94% of the total Fe. There is a weak peak at a position typical of the high-energy line of high-spin Fe(II) (see arrow in Figure 2-7B), which likely bound opportunistically to *Mt*LipA during the reconstitution procedure . The Mössbauer spectrum (4.2-K/53-mT) collected over a wider range of Doppler velocities (data not shown) does not reveal any broad,

magnetically split features. The EPR spectrum of an identical $^{57}$RCN *Mt*LipA sample provides consistent results, revealing no signals and thus ruling out the presence of Fe/S clusters with a $S = ½$ ground state (Figure 2-10). These results, combined with the Fe-S analyses, indicate the presence of 1.83 $[4Fe\text{-}4S]^{2+}$ clusters per RCN *Mt*LipA.

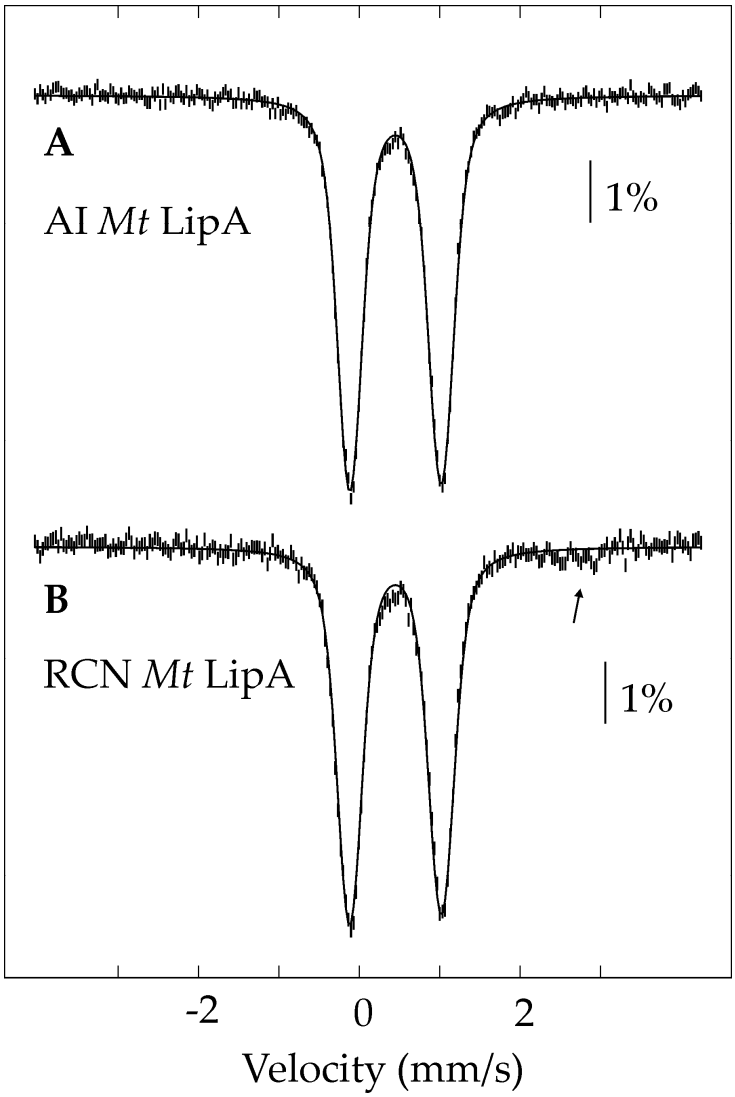


Figure **2-7**: 4.2-K/53-mT Mössbauer spectra of AI *Mt*LipA (vertical bars in A) and RCN *Mt*LipA (vertical bars in B) enhanced with $^{57}$Fe. The spectra are accompanied by a simulated quadrupole doublet with parameters typical of $[4Fe\text{-}4S]^{2+}$ clusters ($\delta$ = 0.45 mm/s and $\Delta E_Q$ = 1.15 mm/s), which accounts for 96 and 94% of the total intensity, respectively (solid lines in A and B). The arrow in B indicates the presence of a high-energy line emanating from a small amount of high-spin Fe(II) in the $^{57}$RCN sample.

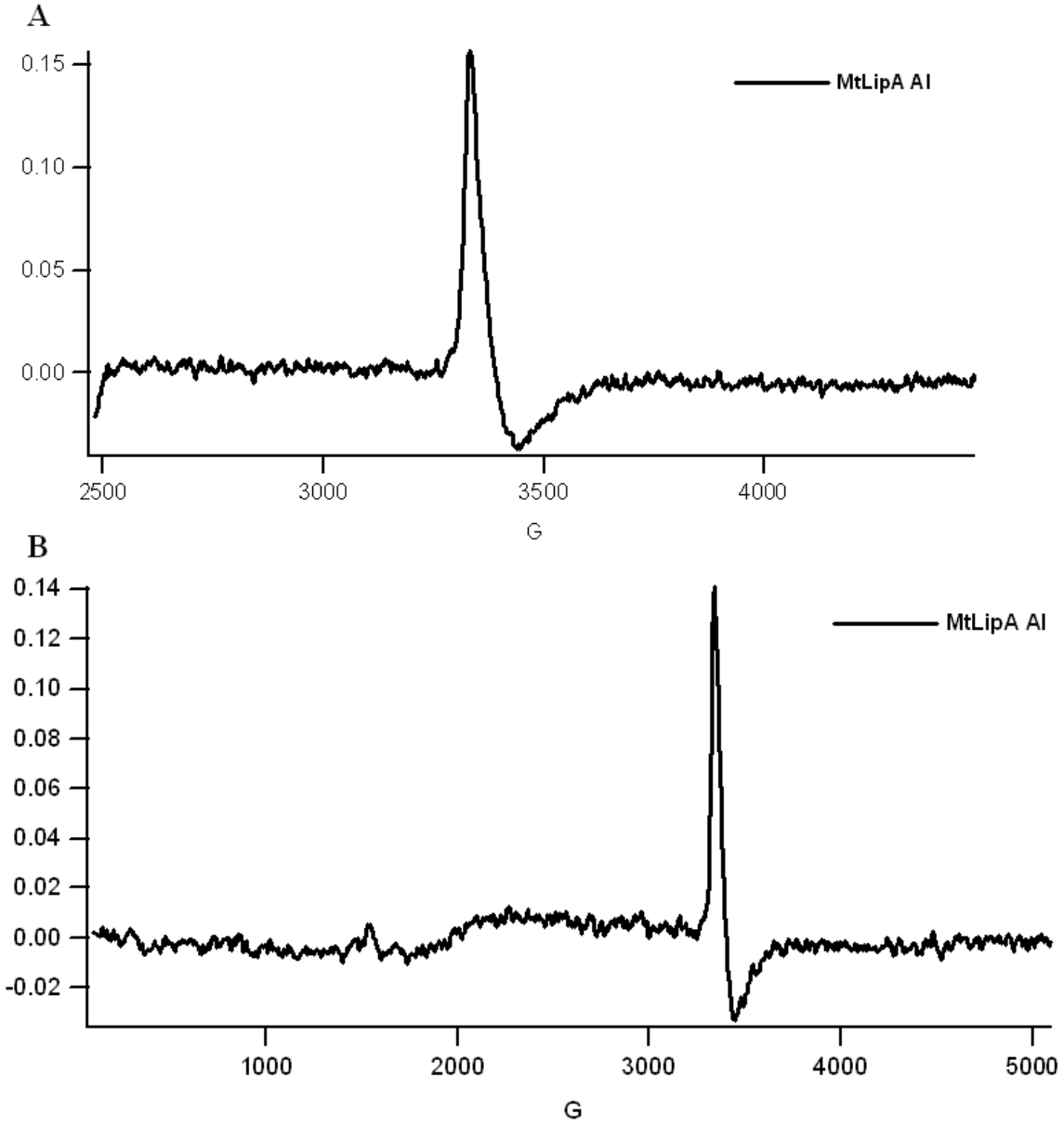


Figure **2-8**: EPR spectra for AI *Mt*LipA samples enhanced with $^{57}$Fe, and run with center field of 3480 Gauss and sweep width of 2000 Gauss (A), and center field of 2600 Gauss and sweep width of 5000 Gauss (B).

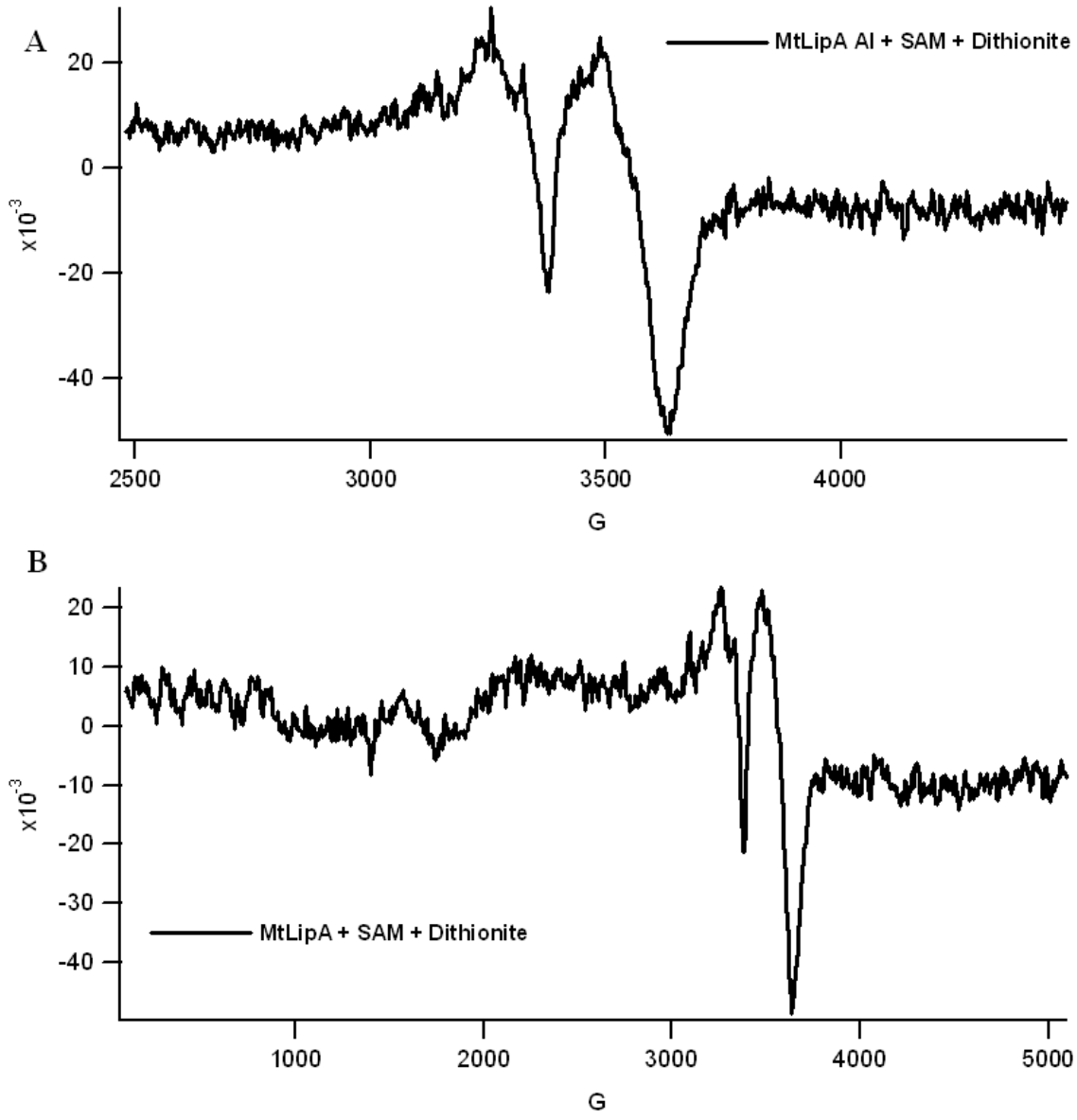


Figure **2-9**: EPR spectra of AI *Mt*LipA samples enhanced with $^{57}$Fe and reduced with dithionite, and run with center field of 3480 Gauss and sweep width of 2000 Gauss (A), and center field of 2600 Gauss and sweep width of 5000 Gauss (B).

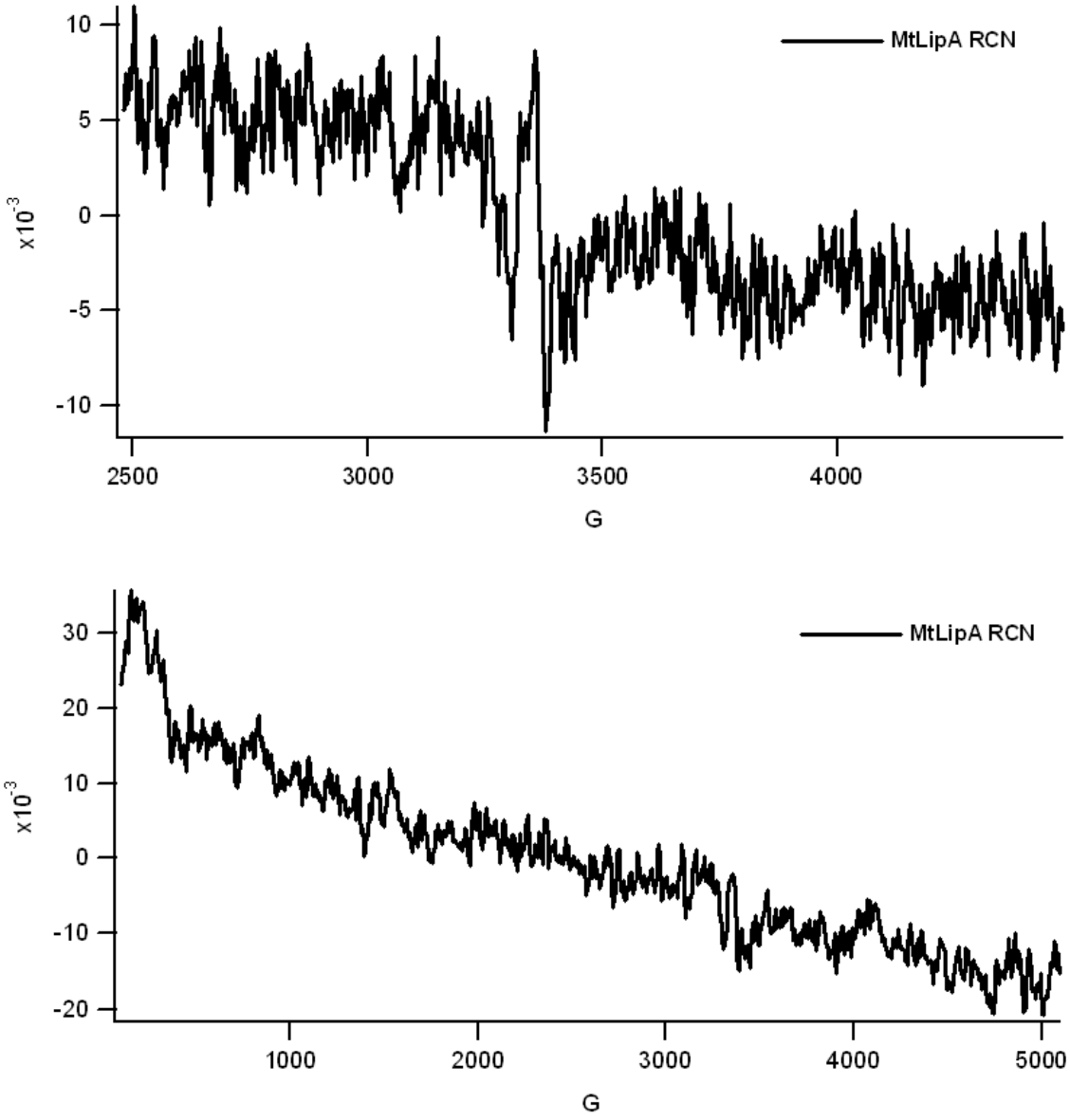


Figure **2-10**: EPR spectra of RCN *Mt*LipA samples enhanced with $^{57}$Fe, and run with center field of 3480 Gauss and sweep width of 2000 Gauss (A), and center field of 2600 Gauss and sweep width of 5000 Gauss (B).

## 2.4 Discussion

LipA polypeptide is an ideal candidate for study, not only because of its membership in the radical SAM superfamily of metalloenzymes, but because it plays a significant catalytic role in an essential pathway: the *de novo* synthesis of the lipoyl cofactor. This cofactor acts as a critical swinging arm in several major metabolic processes in both prokaryotic and eukaryotic cells: the pyruvate dehydrogenase complex, the glycine cleavage system, the α-ketoglutarate dehydrogenase complex, the branched-chain oxo-acid dehydrogenase complex, and the acetoin dehydrogenase complex. LipA has the pivotal role of catalyzing the removal of two hydrogen atoms from a saturated fatty acyl chain, and the insertion of two sulfur atoms in their place (C-6 and C-8) to create the final lipoyl cofactor product. This reaction is initiated through the donation of an electron by the [4Fe-4S] $^{2+}$ cluster of LipA residing in the CXXXCXXC motif, to the sulfonium of a SAM molecule. This causes SAM to break down into methionine and a highly reactive 5'dA• radical; the radical species then goes on to abstract hydrogen from the C-6 of the protein-bound octanoic acid, followed by the insertion of a sulfur atom donated by LipA itself from the CXXXXCXXXXXC Fe-S cluster (86,89). The [4Fe-4S]$^{2+}$ radical-SAM (RS) cluster is re-reduced, and then the reaction proceeds as before, this time with sulfur insertion at C-8. Each 5'dA• is capable of removing one hydrogen molecule from the octanoyl moiety, and thus two equivalents of 5'dA• (and therefore two SAM) are required to produce one equivalent of lipoyl cofactor product (73,81).

This knowledge exists because of a compilation of data from extensive research on the biochemical and mechanistic action of the LipA of *E. coli* in the context of its role

as a SAM superfamily enzyme. However, there is no published data on the LipA protein analog found in *M. tuberculosis*. It is in this organism that LipA becomes of even greater significance, since tubercle bacilli do not possess an alternative lipoyl cofactor synthesis route while *E. coli* does. In other words, without proper LipA activity, tuberculosis bacteria would theoretically not be able to survive due to lipoic acid depletion. It is under this premise that the genes of the proteins responsible for lipoic acid synthesis were cloned, and LipA was subjected to further characterization through spectroscopy, analytical techniques, and activity assays.

The *Mt*LipA behavior and spectral results here for the most part are in accordance with findings to date on *Ec*LipA. The UV-vis spectra of all four protein samples exhibited a dominant peak at 280 nm, a small shoulder around 330 nm and a broader peak around 410 nm that is characteristic of [4Fe-4S] cluster presence (81). This presence was further corroborated by the dark brown color of the protein samples. The $A_{280}/A_{410}$ ratios fell between 2.2 and 3.2; these results are consistent with previous experimentation in the Booker Laboratory on *Ec*LipA that found an $A_{280}/A_{410}$ of 2.88 for AI *Ec*LipA and 2.04 for RCN *Ec*LipA (81).

The Fe and S quantification also gleaned the expected values, assuming *Mt*LipA is structurally analogous to *Ec*LipA. Because LipA has been determined to contain two 4Fe-4S clusters, it is expected that experimentation will reveal 8 Fe and 8 S equivalents per *Mt*LipA protein. The $^{57}$Fe AI and RCN samples were closest to this, containing ~ 7-8 equivalents of Fe and ~ 5-8 of S per monomer – results consistent with work by both Cicchillo *et al*. and Billgren in the Booker Laboratory (81,89). Upon reconstitution, *Mt*LipA did not experience quite as much of an increase in Fe-S content as *Ec*LipA in

previous study (an observed increase of 1-3 equivalents versus an increase of 6-7 equivalents in work by Cicchillo *et al*.), which may be due to either experimental circumstance or the existence of divergent Fe-S incorporation strategies between the two protein analogs. *Ec*LipA is known to attract large amounts of adventitiously bound iron as a consequence of the reconstitution procedure, whereas it is possible that *Mc*LipA does not.

Mössabuer spectroscopy for both $^{57}$AI and $^{57}$RCN samples exhibited spectra typical of [4Fe-4S] $^{2+}$ clusters and congruent with spectra resulting from WT *Ec*LipA in previous experimentation by Cicchillo *et al*. (81). EPR results for both proteins are also in accordance with [4Fe-4S] $^{2+}$ cluster presence, with the exception of a small [3Fe-4S]$^{+}$ presence (~0.4% of the total Fe) indicated in the $^{57}$AI EPR spectrum, commonly observed in AI radical SAM enzymes. These spectral findings, when taken together with the Fe-S quantification results, indicate a stoichiometry of 1.7 [4Fe-4S] $^{2+}$ clusters per AI *Mt*LipA and 1.83 [4Fe-4S] $^{2+}$ clusters per RCN *Mt*LipA. Thus *Mt*LipA, like *Ec*LipA, harbors two [4Fe-4S] clusters: the RS cluster, which is presumably ligated by cysteines 81, 85, and 88 of the hallmark CXXXCXXC motif, and the putative S-donor cluster, which is most likely coordinated by cysteines 55, 60, and 66 of the CXXXXCXXXXXC motif, in analogy to *Ec*LipA.

Lastly, activity assays with octanoyl-peptide measuring generation of 5'dA and lipoyl H-protein yielded the expected results for an analog of *Ec*LipA functioning in circumstances of partial turnover. Lipoyl H-protein product, which was generated to a final concentration of approximately half the starting concentration of *Mt*LipA, suggested that in this reaction mixture *Mt*LipA was only able to cleave a single SAM molecule *in*

*vitro* due to its self-destruction during catalysis. This would presumably require two *Mt*LipA proteins to produce one lipoyl H-protein product. However, 5'dA, a byproduct of SAM catabolism, was generated in amounts to suggest more than one equivalent was produced per *Mt*LipA, indicating that re-reduction of protein, though not occurring at an optimal rate, was taking place to some extent.

Of note were the difficulties encountered during the cloning of the *M. tuberculosis* genes, which resulted in the necessity of several different PCR attempts. This can likely be attributed to the high guanine-cytosine (GC) base pair content in the *M. tuberculosis* genome, as well as in two of the three genes chosen, *lipa* and *lipb* (25). GC-rich base pair sequences cause difficulties during PCR cloning because they create strong secondary DNA structure that is resistant to denaturation, preventing primer annealing (92). This was only overcome in this experiment after the polymerase in use (Vent) was replaced by PfuTurbo polymerase, which may have superior performance with GC-rich targets because it contains ArchaeMaxx, which functions as a dUTPase (93). dUTP accumulation during PCR occurs through dCTP deamination and inhibits PCR performance (94).

## 2.5 Conclusion

In summation, we have herein provided evidence to suggest that *Mt*LipA is analogous to *Ec*LipA with regard to its 2 $[4Fe\text{-}4S]^{2+}$ cluster catalytic center and its basic activity in the presence of substrate. This study marks the beginning of investigations into *Mt*LipA, with the intent to evaluate and explore its potential as a

future target for anti-TB antibiotics. Because so much has already been elucidated about *Ec*LipA (*Mt*LipA's presumed analog), and because human cells possess an alternate lipoic acid synthesis pathway not available to tuberculosis mycobacterium, *Mt*LipA merits further work. The most powerful antibiotics in the world can arise from a single inhibitory function; perhaps stopping *Mt*LipA action is what will finally bring the tuberculosis epidemic to its knees.

# REFERENCES


1. Mendez, J. (2001). Multi drug resistance in tuberculosis and the use of PCR for defining molecular markers of resistance. *Jacksonville Medicine*.
2. Abbate, E., Vescovo, M., Natiello, M., Cufré, M., & García, A. (2007). Tuberculosis extensamente resistente (XDR-TB) en Argentina: aspectos destacables epidemiológicos, bacteriológicos, terapéuticos y evolutivos. *Revista argentina de medicina respiratoria*, *7*(1).
3. Colditz, G., Brewer, T., Berkey, C., Wilson, M., Burdick, E., Fineberg H., Mosteller, F. (1994). Efficacy of bcg vaccine in the prevention of tuberculosis. meta-analysis of the published literature.. *Journal of the American Medical Association*, *271*(9), 698-702.
4. van Soolingen, D., de Haas, P., Hermans, P., Groenen, P., & van Embden, J. (1993). Comparison of various repetitive DNA elements as genetic markers for strain differentiation and epidemiology of *Mycobacterium tuberculosis*. *Journal of Clinical Microbiology*, *31*(8), 1987-95.
5. van Embden, J., van Soolingen, D., Small, P., & Hermans, P. (1992). Genetic markers for the epidemiology of tuberculosis. *Respiratory Microbiology*, *143*(4), 385-91.
6. Rastogi, N, & McFadden, J.J. (1992). Mycobacteria and aids: epidemiological and genetic markers, virulence factors and interactions with the immune system.. *Research In Microbiology*, *143*(4), 361-362.
7. Kapur, V., Whittam, T., & Musser, J. (1994). Is *Mycobacterium tuberculosis* 15,000 years old?. *The Journal of Infectious Diseases*, *170*(5), 1348-1349.
8. Somoskovi, A, Dormandy, J, Rivenburg, J, Pedrosa, M, McBride, M., & Salfinger, M. (2008). Direct comparison of the genotype MTBC and genomic deletion assays in terms of ability to distinguish between members of the *Mycobacterium tuberculosis* complex in clinical isolates and in clinical specimens. *Journal of Clinical Microbiology*, *46*(5), 1854-1857.
9. Smith, I. (2003). *Mycobacterium tuberculosis* pathogenesis and molecular determinants of variance. *Clinical Microbiology Reviews*, *16*(3), 463-496.
10. Böddinghaus, B, Rogall, T, Flohr, T, Blöcker, H, & Böttger, E. (1990). Detection and identification of mycobacteria by amplification of rRNA. *Journal of Clinical Microbiology*, *28*(8), 1751-1759.
11. Cockburn, A. (1964). The Evolution and eradication of infectious disease. *The American Journal of Tropical Medicine and Hygiene*, *13*(4), 651-652.
12. Streevatsan, S., Pan, X., Stockbauer, K., Connell, N., & Kreiswirth, B.. (1997). Restricted structural gene polymorphism in the *Mycobacterium tuberculosis* complex indicated evolutionarily recent global dissemination. *Proceedings of the National Academy of Sciences of the United States of America*, *94*, 9869-9874.
13. Brosch, R., S. V. Gordon, M. Marmiesse, P. Brodin, C. Buchrieser, K. Eiglmeier, T. Garnier, C. Gutierrez, G. Hewinson, K. Kremer, L. M. Parsons, A. S. Pym, S. Samper, D. van Soolingen, and S. T. Cole. (2002). A new evolutionary scenario

for the *Mycobacterium tuberculosis* complex. *Proceedings of the National Academies of Science USA*, (99)**,** 3684-3689.

14. Zink, A., Sola, C., Reischl, U., Grabner, W., Rastogi, N., Wolf, H., Nerlich, G. (2003). Characterization of *Mycobacterium tuberculosis* complex DNAs from Egyptian mummies by spoligotyping. *Journal of Clinical Microbiology*, *41*(1), 359-367.
15. History of Tuberculosis. (2007). *Nebraska department of health & human services*. Retrieved (2010, March 7) from http://www.hhs.state.ne.us/cod/Tuberculosis/TBHistory.htm
16. Kaufmann, S. (2000). Robert Koch's highs and lows in the search for a remedy for tuberculosis. *Nature Medicine*, Retrieved from http://www.nature.com/nm/focus/tb/historical_perspective.html
17. Schatz, A., & Waksman, S. A. (1944). Effect of streptomycin and other antibiotic substances upon *Mycobacterium tuberculosis* and related organisms. *Proceedings of the Society for Experimental Biology and Medicine*, *57*, 244-248.
18. Lehman, J. (1946). Para-aminosalacylic acid in the treatment of tuberculosis. *Lancet*, *i*(15).
19. Gillespie, S. (2002). Evolution of drug resistance in *Mycobacterium tuberculosis*: clinical and molecular perspective. *Antimicrobial Agents and Chemotherapy*, *46*(2), 267-274.
20. Crofton, J, & Mitchison, D. (1948). Streptomycin resistance in pulmonary tuberculosis. *British Medical Journal*, *2*, 1009-1015.
21. Parsons, L., Driscoll, J., Taber, H., & Salfinger, M. (1997). Drug resistance in tuberculosis. *Infectious Disease Clinics of North America*, *11*(4).
22. Alderwick, L, Birch, H, Mishra, A, Eggeling, L, & Besra, G. (2007). Structure, function and biosynthesis of the *Mycobacterium tuberculosis* cell wall: arabinogalactan and lipoarabinomannan assembly with a view to discovering new drug targets. *Biochemical Society Transactions*, *35*(5), 1325-1328.
23. Brennan, P.J. (2003). Structure, function, and biogenesis of the cell wall of *Mycobacterium tuberculosis*. *Tuberculosis (Edinb)*, *83*(1-3), 91-97.
24. Jarlier, V., & Nikaido, H. (1994). Mycobacterial cell wall: structure and role in natural resistance to antibiotics. *FEMS Microbiology Letters*, *123*(1-2), 11-18.
25. Todar, K. (2009). *Online textbook of bacteriology - Mycobacterium tuberculosis and tuberculosis*, Retrieved from http://www.textbookofbacteriology.net/tuberculosis.html
26. Katti, M., Hunter, R., & Jagannath, C. (2003). Trehalose dimycolate (cord factor) from *Mycobacterium tuberculosis* modulates macrophage function through activation of focal adhesion kinase. *Abstracts From the 43rd Interscience Conference on Antimicrobial Agents and Chemotherapy*.
27. Finken, M., Kirschner, P., Meier, A., Wrede, A., & Böttger, E. (2006). Molecular basis of streptomycin resistance in *Mycobacterium tuberculosis*: alterations of the ribosomal protein s12 gene and point mutations within a functional 16s ribosomal RNA pseudoknot. *Molecular Microbiology*, *9*(6), 1239-1246.
28. Scheindlin, S. (2006). The Fight against tuberculosis. *Molecular Interventions*, *6*(3), 124-130.

29. Takayama, K, Schnoes, H, Armstrong, E, & Boyle, R. (1975). Site of inhibitory action of isoniazid in the synthesis of mycolic acids in *Mycobacterium tuberculosis*. *The Journal of Lipid Research*, *16*, 308-317.
30. Banerjee, A, Dubnau, E, Quemard, A, Balasubramanian, V, Um, K., Wilson, T., Collins, D., de Lisle, G., & Jacobs, W. (1994). Inha, a gene encoding a target for isoniazid and ethionamide in *Mycobacterium tuberculosis*. *Science*, *263*(5144), 227-230.
31. Barry, C, & Mdluli, K. (1996). Drug sensitivity and environmental adaptation of mycobacterial cell wall components. *Trends in Microbiology*, *4*(7), 275-281.
32. Cordice, J, Hill, L, & Wright, L. (1953). Use of Pyrazinamide (aldinamide) in the treatment of tuberculosis lymphadenopathy and draining sinuses. *Journal of the National Medical Association*, *45*(2), 87-98.
33. Zhang, Y, Permar, S, & Sun, Z. (2002). Conditions that may affect the results of susceptibility testing of *Mycobacterium tuberculosis* to pyrazinamide. *Journal of Medical Microbiology*, *51*, 42-49.
34. Zhang, Y, Wade, M, Scorpio, A, Zhang, H, & Sun, Z. (2003). Mode of action of pyrazinamide: disruption of *Mycobacterium tuberculosis* membrane transport and energetics by pyrazinoic acid. *Journal of Antimicrobial Chemotherapy*, *52*, 790-795.
35. Mitchison, D. (1985). The Action of antituberculosis drugs in short-course chemotherapy. *Tubercle*, *66*, 219-225.
36. Unissa, A, Selvakumar, N, & Hassan, S. (2009). Insight to pyrazinamide resistance in *Mycobacterium tuberculosis* by molecular docking. *Bioinformation*, *4*(1), 24-29.
37. Sensi, P., Greco, A.M., & Ballotte, R. (1960). Rifomycin I. Isolation and properties of Rifomycin B and Rifomycin Complex. *Antibiotics Annual 1959–1960*. New York, Antibiotica, Inc., 262–270.
38. Lorian, V, & Finland, M. (1969). In vitro effect of rifampin on mycobacteria. *Applied Microbiology*, *17*(2), 202-207.
39. Miller, L, Crawford, J, & Shinnick, T. (1994). The *Rpob* gene of *Mycobacterium tuberculosis*. *Antimicrobial Agents and Chemotherapy*, *38*(4), 805-811.
40. Somoskovi, A, Parsons, L, & Salfinger, M. (2001). The Molecular basis of resistance to isoniazid, rifampin, and pyrazinamide in *Mycobacterium tuberculosis*. *Respiratory Research*, *2*, 164-168.
41. Sandman, L, Schluger, N, Davidow, A, & Bonk, S. (1999). Risk factors for rifampin-monoresistant tuberculosis : a case-control study. *American Journal of Respiratory and Clinical Care Medicine*, *159*(2), 468-472.
42. Wilkinson, R, Shepherd, R, Thomas, J, & Baughn, C. (1961). Stereospecificity in a new type of synthestic antituberculosis agent. *Journal of the American Chemical Society*, *83*(9), 2212-2213.
43. Telenti, A, Philipp, W, Sreevatsan, S, Bernasconi, C, & Stockbauer, K. (1997). The Emb operon, a gene cluster of *Mycobacterium tuberculosis* involved in resistance to ethambutol. *Nature Medicine*, *3*, 567-570.

44. Takayama, K, & Kilburn, J. (1989). Inhibition of synthesis of arabinogalactan by ethambutol in mycobacterium smegmatis. *Antimicrobial Agents and Chemotherapy*, *33*(9), 1493-1499.
45. Wolucka, B, McNeil, M, de Hoffman, E, Chojnacki, T, & Brennan, P. (1994). Recognition of the lipid intermediate for arabinogalactan/arabinomannan biosynthesis and its relation to the mode of action of ethambutol on mycobacteria. *Journal of Biological Chemistry*, *269*, 23328-23335.
46. Belanger, A.E., Besra, G.S., Ford, M.E., Mikusová, K., Belisle, J.T., Brennan, P.J., & Inamine, J.M. (1996). The *embAB* genes of *Mycobacterium avium* encode an arabinosyl transferase involved in cell wall arabinan biosynthesis that is the target for the antimycobacterial drug ethambutol. *Proceedings of the National Academy of Sciences of the United States of America*, 93, 11919−11924.
47. Kaufmann, S. (2000). Is the Development of a new tuberculosis vaccine possible?. *Nature Medicine*, *6*, 955-960.
48. Position paper on BCG vaccination. (2004). *WHO Weekly epidemiological record*, *79*(4), 25-40.
49. Fine, P.E. (1995). Variation in protection by BCG: implications of and for heterologous immunity. *Lancet*, *346*(8986), 1339-1345.
50. Lin, M.Y, & Ottenhoff, T.H. (2008). Not to wake a sleeping giant: new insights into host-pathogen interactions identify new targets for vaccination against latent *Mycobacterium tuberculosis* infection. *Biological Chemistry*, *389*(5), 497-511.
51. (2006). Tuberculosis: a global emergency. *The National Foundation for Infectious Disease*. Retrieved from http://www.nfid.org/factsheets/tb.shtml.
52. (2010). Drug- and multidrug-resistant tuberculosis (MDR-TB). *The World Health Organization*, Retrieved from http://www.who.int/tb/challenges/mdr/en/index.html.
53. Reed, L.R. (1974). Multienzyme complexes. *Accounts of Chemical Research*, *7*, 40-46.
54. Kresge, N, Simoni, R, & Hill, R. (2006). Lester j. reed and the α-keto acid dehydrogenase complexes. *The Journal of Biological Chemistry*, *238*, 30-39.
55. Gunsalus, C., Struglia, L., & O'Kane, D. (1952). Pyruvic acid metabolism: IV. Occurrence, properties, and partial purification of pyruvate oxidation factor. *The Journal of Biological Chemistry*, *194*, 859-869.
56. Reed, L.J. (2001). A Trail of research from lipoic acid to α-keto acid dehydrogenase complexes. *The Journal of Biological Chemistry*, *276*, 38329-38336.
57. Reed, L.J, Gunsalus, I.C, Schnakenberg, G.H.F, Soper, Q.F, Boaz, H.E., Kern, S.F., Parke, T.V. (1953). Isolation, characterization and structure of alpha-lipoic acid. *Journal of the American Chemical Society*, *75*(6), 1267-1270.
58. Raddatz, G, & Bisswanger, H. (1997). Receptor site and stereospecifity of dihydrolipoamide dehydrogenase for r- and s-lipoamide: a molecular modeling study . *Journal of Biotechnology*, *58*(2), 89-100.
59. Koike, M, & Reed, L.J. (1960). α-keto acid dehydrogenation complexes: ii. the role of protein-bound lipoic acid and flavin adenine dinucleotide . *Journal of Biological Chemistry*, *235*, 1931-1938.

60. Biewenga, G.P, Haenen, G.R, & Bast, A. (1997). The Pharmacology of the antioxidant lipoic acid. *General Pharmacology*, *29*(3), 315-331.
61. Reed, L.J, Koike, M, Levitch, M.E, & Leach, F.R. (1958). Studies on the nature and reactions of protein-bound lipoic acid . *The Journal of Biological Chemistry*, *232*, 143-158.
62. Kikuchi, G. (1973). The Glycine cleavage system: composition, reaction mechanism, and physiological significance. *Molecular & Cellular Biochemistry*, *1*(2), 169-187.
63. Kikuchi, G, & Hiraga, K. (1982). The Mitochondrial glycine cleavage system. *Molecular & Cellular Biochemistry*, *45*(3), 137-149.
64. Pettit, F., Hamilton, L., Munk, P., Namihira, G., Eley, M., Willms, C., & Reed, L.J. (1973). Aceto acid dehydrogenase complexes. *The Journal of Biological Chemistry*, *248*(15), 5282-5290.
65. Meixner-Monori, R, Kubicek, C.P, Habison, A, Kubicek-Pranz, E.M, & Röhr, M. (1985). Presence and regulation of the alpha-ketoglutarate dehydrogenase multienzyme complex in the filamentous fungus aspergillus niger.. *Journal of Bacteriology*, *161*(1), 265-271.
66. Patel, M.S, & Packer, L. (2008). *Lipoic acid: energy production, antioxidant activity and health effects*. Boca Raton, FL: CRC Press.
67. Payne, K.A, Hough, D.W, & Danson, M.H. (2010). Discovery of putative acetoin dehydrogenase complex in the hypermophilic archaeon sulolobus solfataricus. *FEBS Letters [Epub ahead of print]*, Retrieved from http://www.ncbi.nlm.nih.gov.
68. Perham, R.N. (2000). Swinging arms and swinging domains in multifunctional enzymes: catalytic machines for multistep reactions. *Annual Review of Biochemistry*, *69*, 961-10004.
69. Rock, C. (2009). Opening a new path to lipoic acid. *Journal of Bacteriology*, *191*(22), 6782-6784.
70. Morris, T.W, Reed, K.E, & Cronan, J.E. (1995). Lipoic acid metabolism in Escherichia coli: the lpla and lipb genes define redundant pathways for ligation of lipoyl groups to apoprotein. *Journal of Bacteriology*, *177*, 1-10.
71. Fujiwara, K., Takeuchi, S., Okamura-Ikeda, K., & Motokawa, Y. (2001). Purification, characterization, and cDNA cloning of lipoate-activating enzyme from bovine liver cDNA. *The Journal of Biological Chemistry*, *276*, 28819-28823.
72. Ma, Q, Zhao, X, Eddine, A.N, Geerlof, A, Li, X., Cronan, J.E., Kaufmann, S., Wilmanns, M. (2006). The *Mycobacterium tuberculosis* Lipb enzyme functions as a cysteine/lysine dyad acyltransferase. *Proceedings of the National Academy of Sciences*, *103*(23), 8662-8667.
73. Cicchillo, R.M, Iwig, D.F, Jones, A.D, Nesbitt, N.M, Beleanu-Gogonea, C., Souder, M.G., Tu, L., & Booker, S.J. (2004). Lipoyl synthase requires two equivalents of s-adenosyl-l-methionine to synthesize one equivalent of lipoic acid. *Biochemistry*, *43*, 6378-6386.
74. Vanden Boom, T.J, Reed, K.E, & Cronan, J.E. (1991). Lipoic acid metabolism in *Escherichia* coli: isolation of null mutants defective in lipoic acid biosynthesis,

molecular cloning and characterization of the e. coli lip locus, and identification of the lipoylated protein of the glycine cleavage system.. *The Journal of Bacteriology*, *173*, 6411-6420.

75. Reed, K.E, Morris, T.W, & Cronan, J.E. (1994). Mutants of *Escherichia* coli k-12 that are resistant to a selenium analog of lipoic acid identify unknown genes in lipoate metabolism. *The Proceedings of the National Academy of the Sciences of the USA*, *91*, 3720-3724.
76. Sassetti, C.M, Boyd, D.H, & Rubin, E.J. (2003). Genes required for mycobacterial growth defined by high density mutagenesis. *Molecular Microbiology*, *48*(1), 77-84.
77. Rachman, H, Strong, M, Ulrichs, T, Grode, L, & Schuchhardt, J. (2006). Unique transcriptome signature of *Mycobacterium tuberculosis* in pulmonary tuberculosis. *Infection and Immunology*, *74*(2), 1233-1242.
78. Hayden, M.A, Huang, I, Bussiere, D.E, & Ashley, G.W. (1992). The Biosynthesis of lipoic acid. cloning of lip, a lipoate biosynthetic locus of *Escherichia* coli. *Journal of Biological Chemistry*, *267*, 9512-9515.
79. Reed, K.E, & Cronan, J.E. (1993). Lipoic acid metabolism in *Escherichia* coli: sequencing and functional characterization of the lipa and lipb genes. *Journal of Bacteriology*, *175*, 1325-1336.
80. Busby, R, Schelvis, J, Yu, D, Babcock, G, & Marletta, M. (1999). Lipoic acid biosynthesis: lipa is an iron-sulfur protein. *Journal of the American Chemical Society*, *121*(19), 4706-4707.
81. Cicchillo, R, Lee, K.H, Baleanu-Gogonea, C, Nesbitt, N.M, & Krebs, C. (2004). Escherichia coli lipoyl synthase binds two distinct [4Fe-4S] clusters per polypeptide. *Biochemistry*, *43*, 11770-11781.
82. Frey, P.A, Hegeman, A.D, & Ruzicka, F.J. (2008). The Radical SAM superfamily. *Critical Reviews in Biochemistry and Molecular Biology*, *43*(1), 63-88.
83. Walsby, C.J, Ortillo, D, Broderick, W.E, Broderick, J.B, & Hoffman, B.M. (2002). An Anchoring role for FeS clusters: chelation of the amino acid moiety of s-adenosylmethionine to the unique iron site of the [4Fe−4S] cluster of pyruvate formate-lyase activating enzyme. *Journal of the American Chemical Society*, *124*(38), 11270-11271.
84. Challand, M, Ziegert, T, Douglas, P, Wood, R, & Kriek, M. (2009). Product inhibition in the radical s-adenosylmethionine family. *FEBS Letters*, *583*(8), 1358-1362.
85. Booker, S.J, Cicchillo, R.M, & Grove, T.L. (2007). Self sacrifice in radical s-adenosylmethionine proteins. *Current Opinion in Chemical Biology*, *11*(5), 543-552.
86. Cicchillo, R.M, & Booker, S.J. (2005). Mechanistic investigations of lipoic acid biosynthesis in *Escherichia coli*: both sulfur atoms in lipoic acid are contributed by the same lipoyl synthase polypeptide. *Journal of the American Chemical Society*, *127*(9), 2860-2861.
87. Schomburg, & Schomburg. (2009). *Springer handbook of enzymes*. Berlin: Springer.

88. Steiert, P, Stauffer, L, & Stauffer, G. (1990). The *Lpd* gene product functions as the l protein in the *Escherichia coli* glycine cleavage enzyme system. *Journal of Bacteriology*, *172*(10), 6142-6144.
89. Billgren, E. (2008). Mechanistic investigation of the *Echerichia coli* lipoyl synthase. *The Pennsylvania State University*.
90. Kent, T.A., Huynh, B.H., & Münck, E. (1980). Iron-sulfur proteins: spin-coupling model for three-iron clusters . *Proceedings of the National Academy of Sciences*, *77*(11), 6574-6576.
91. Krebs, C, Henshaw, T, Cheek, J, Huynh, B, & Broderick, J. (2000). Conversion of 3Fe-4S to 4Fe-4S clusters in native pyruvate formate-lyase activating enzyme: Mössbauer characterization and implications for mechanism. *Journal of the American Chemical Society*, *122*(50), 12497–12506.
92. Majlingovà, P, Paroncini, P, Svegliati, S, Luchetti, M, & Gabrielli, A. (2003). Successful PCR amplification and subcloning of a GC-rich DNA fragment. *QIAGEN News*, (1), 18-19.
93. Pfuturbo® dna polymerase: instruction manual. La Jolla: Stratagene.
94. Hogrefe, H, Hansen, C, Scott, B, & Nielson, K. (2002). Archaeal dUTPase enhances PCR amplifications with Archaeal DNA polymerases by preventing dUTP incorporation. *Proceedings of the National Academy of Sciences*, *99*(2), 596-601.
95. Spalding, M, & Prigge, S. (2010). Lipoic acid metabolism in microbial pathogens. *Microbiology and Molecular Biology Reviews*, *74*(2), 200-228.

# - Abigail Horstmann -


616 West College Ave., Apt. #3,
State College, PA, 16801
(914)-474-8275
akh5036@psu.edu

255 Rombout Road,
Pleasant Valley, NY, 12569
(845)-635-2654
abby.horstmann@gmail.com


## Education:

Pennsylvania State University – Scholar of the Schreyer Honors College
BS in Biochemistry and Molecular Biology, Minor in Spanish
Expected graduation date: 08/2010
GRE scores: 790 Math, 760 Verbal

**Related coursework:**

| | | |
|---|---|---|
| General Chemistry I & II | Antibiotic Resistance | Biochemistry I, II, III, IV |
| Organic Chemistry I & II | Biology I, II, & III | Genetic Analysis |
| Physical Chemistry I & II | Physics I, II, & III | Molecular Medicine |

## Work Experience:

**Booker Lab – PSU Biochem. Dept. (January 2009 – present):** *Research Assistant*
Worked with students/faculty 10-15 hrs/wk with the goal of characterizing an enzymatic pathway of *Mycobacterium tuberculosis* as a potential antibiotic target. Conducted PCR, bacterial transformations and culturing, DNA extraction, and protein expression analysis.

**Light Knowledge Resources (September 2009 – present):** *Writing Intern*
Wrote 1-2 articles/week on HIV/AIDS news, research, and issues, in a format accessible to the public. Work published on the AIDS Beacon website.

**Keystone Nano (May 2009 – August 2009):** *Research Intern*
Assisted in development of nanoparticles designed to encapsulate cell therapeutics, extensive use of gel electrophoresis, spectrophotometer analysis, enzyme digestion and sterile technique.

**JRS Pharma (May 2008 – August 2008):** *Research and Development Intern*
Performed physical and chemical tests on excipients, researched and applied the Kjeldahl Nitrogen Determination Method to pilot product.

## Honors and Activities:

Dean's List: Fall 2006, Spring 2007, Fall 2008, Spring 2009, Fall 2009, Spring 2010
Awarded Holmes Teas Chemistry Scholarship at Penn State
Recipient of the Thomas J. Watson Memorial Scholarship
Member of Atlas THON and THON Hospitality
Two-time participant in the Appalachian Service Project